Theory of Cation Solvation and Ionic Association in Nonaqueous Solvent Mixtures

Zachary A.H. Goodwin[1,2,*] Michael McEldrew[3] Boris Kozinsky[2,4] and Martin Z. Bazant[3,5]

[1]*Department of Materials, Imperial College of London, South Kensington Campus, London SW7 2AZ, United Kingdom*

[2]*John A. Paulson School of Engineering and Applied Sciences, Harvard University, Cambridge, Massachusetts 02138, USA*

[3]*Department of Chemical Engineering, Massachusetts Institute of Technology, Cambridge, Massachusetts USA*

[4]*Robert Bosch LLC Research and Technology Center, Cambridge, Massachusetts 02139, USA*

[5]*Department of Mathematics, Massachusetts Institute of Technology, Cambridge, Massachusetts, USA*

Conventional lithium-ion batteries, and many next-generation technologies, rely on organic electrolytes with multiple solvents to achieve the desired physicochemical and interfacial properties. The complex interplay between these properties can often be elucidated via the coordination environment of the cation. We develop a theory for the coordination shell of cations in nonaqueous solvent mixtures that can be applied with high fidelity, up to extremely high salt concentrations. Our theory can naturally explain simulation and experimental values of cation solvation in "classical" nonaqueous electrolytes. Moreover, we utilize our theory to understand general design principles of emerging classes of nonaqueous electrolyte mixtures, such as high entropy electrolytes. It is hoped that this theory provides a systematic framework to understand simulations and experiments that engineer the solvation structure and ionic associations of concentrated nonaqueous electrolytes.

I. INTRODUCTION

Lithium-ion batteries (LIBs) have transformed our everyday lives through myriad portable electronic devices [1–8]. Although current LIBs are tremendously successful, further development is necessary to meet safety and performance requirements for widespread use of electric vehicles and grid-level energy storage of renewable energy [4–8]. Thus, much of electrochemical energy storage research is focused on improving the materials beyond commercial LIBs, including high-voltage and high-capacity cathode materials [9], silicon anodes [10], lithium metal anodes [11–13], and even non-lithium-based battery chemistries [14–16]. A requirement of any next-generation battery chemistry is an electrolyte that can operate safely, efficiently, and reversibly over the course of the battery's lifetime [1–8].

One of the primary design concepts in electrolyte engineering is balancing desired, often seemingly conflicting, physicochemical properties, such as low viscosity and high conductivity, with interfacial properties, such as low charge transfer resistance and electrode passivation [4]. Commercial LIBs accomplish this design concept, to some extent, with blends of linear carbonates, such as dimethyl carbonate (DMC) for low viscosity, and cyclic carbonates, such as ethylene carbonate (EC) to passivate carbonaceous anodes [1–8,17]. Although carbonate blends provide a serviceable solution, electrolyte design for LIBs is far from optimized [4–8].

An important advance in electrolyte engineering over the past decade has been the link of ion solvation chemistry to electrolyte properties [8,18–23]. On the one hand, at low salt concentrations, solvent-dominated coordination shells ensure nearly complete dissociation of salt, enabling efficient ion transport. However, even at low concentrations, when multiple types of solvent are used, a cation's solvation structure can be tuned via the bulk solvent ratios to produce very different solid-electrolyte interphases (SEIs) to passivate the working electrodes [19]. This is in large part due to the increased reactivity, from reduced LUMO levels, of solvent molecules that are in direct contact with lithium. At higher salt concentrations, the

*zachary.goodwin13@imperial.ac.uk

introduction of anions to the coordination shell tends to decrease ionic conductivity and increase concentration overpotentials [1,2]. However, in some cases, highly passivating inorganic anion-derived (as opposed to solvent-derived) SEIs can form, resulting in an overall increase in cell performance [24]. Furthermore, across all salt concentrations and solvent ratios, the solvation dynamics governing charge transfer resistance will be subject to large changes depending on the species comprising the coordination shell of cations [7,8].

In fact, next-generation electrolytes are engineered to tune the solvation shell of cations, and therefore, physicochemical and interfacial properties of the electrolytes [4–8,13,25]. For example, localized high-concentration electrolytes (LHCEs) [14–16,26–29] use typical anions, such as fluorosulfonimide, in high ratios with ether solvents that historically showed promising compatibility with lithium metal anodes, such as 1,2-dimethoxyethane, but which are notoriously limited in terms of oxidative stability [30–33]. The singular aspect of LHCEs is their use of diluents, generally in the form of fluorinated ethers, which are nonsolvating, but highly oxidatively stable [14–16,26–29]. Thus, the nonfluorinated solvent and anion are mostly retained in the lithium coordination shell, where it has enhanced oxidative stability, while the fluorinated ether diluent strictly appears outside of the lithium coordination shell, serving to lubricate the electrolyte (decrease viscosity) while remaining stable [14–16,26–29]. However, a major issue in engineering such next-generation electrolytes is knowing exactly how the solvation shell of the cations will be effected by the *mixtures* that are created to balance the physicochemical and interfacial properties, as they are often not just an average of their neat properties.

To probe the solvation structure of electrolytes, spectroscopic techniques [1,2,8], such as Fourier-transform infrared [34], Raman [35–37], nuclear magnetic resonance [38], and mass spectrometry [19,39], have been employed to give some insight. However, atomistic simulations, including classical molecular dynamics (MD) [19,40–51] and density functional theory (DFT) [35,44,50–52], are typically relied on to give detailed insight into ion solvation. An advantage of DFT is predicting HOMO and LUMO levels of different species, and, therefore, their expected reactivity, in addition to understanding the spectra from different techniques [35]. However, DFT is computationally expensive, and often limited to short length and time scales (when performing *ab initio* MD) [52]. To reach larger scales, classical MD simulations are indispensable in understanding solvation structures and dynamics of ions, but the accuracy and fidelity of the force field often comes under question [19,40–51]. Recent advances in machine learning force fields could offer the accuracy of DFT with the time and length scales of classical force fields [53,54]. However, a systematic way to report solvation structures has not emerged, with practically

every study reporting results in a different way, making it difficult to compare works systematically [6]. Moreover, atomistic simulations can make predictions of specific systems, but they are not able to provide a general understanding that a simple, analytical theory often does.

In this paper, we develop a theory for the solvation structure and ionic associations of concentrated nonaqueous electrolytes. This theory is based on the recent generalization by McEldrew *et al.* [55–58] of the work of Flory [59–64], Stockmayer [65–67], and Tanaka [68–76] on reversible aggregation and gelation in polymer systems to concentrated electrolytes. Our theory only has a handful of physically transparent parameters, all of which can be obtained directly from atomistic simulations. To demonstrate this parameterization, we perform MD simulations of a "classical" nonaqueous electrolyte, 1M LiPF$_6$ in a mixture of ethylene carbonate and propylene carbonate and compare the results to our theory. Overall, our theory is able to naturally explain the solvation structure of this electrolyte for all the studied mixtures. Having benchmarked our theory against a well-studied system, we utilize "toy models" of our theory to understand the design principles of emerging, next-generation LIB electrolytes. The theory is able to provide a depth of understanding, which is indispensable in aiding design principles of these electrolytes. Moreover, the theory provides a systematic framework for simulation techniques to report their results, which we hope will be adopted to bring more transparency to the field.

II. THEORY

The central idea that the presented work is based on is the analogy between concentrated electrolytes and polymers. In concentrated electrolytes, past the Kirkwood transition [77], electrostatic correlations between ions causes the aggregation of ions into structures with alternating spatial order of oppositely charged ions [55,78]. Conceptually, this is similar to the formation of an alternating copolymer of two monomers. The realization of this analogy actually has a long history, with one of the first connections being the similarity between the liquid-vapour phase diagram of ions in their high-temperature gas state and the phase diagram of polymers in solution, as first discussed from a general stand point by Pitzer [79,80]. Simulations of the phase behavior of ions, based on the so-called restricted primitive model [81], have directly revealed the formation of chains of ions [82,83], although this effect has not been quantified in relation to understanding the shape of the phase boundary. The resemblance of these phase diagrams is thought to occur because of the similarity between polymers and fluids of dipolar particles [84,85] that self-assemble into dynamic polymer chains ("equilibrium polymers"), and also between dipolar fluids

and ionic fluids, owing to the association of ions into dipolar and multipolar clusters [84,86]. There are also many examples of the observation of chains, rings, and branched ionic aggregates, amongst other morphologies, forming in simulations of electrolytes [82,83,87–94].

Here, as in our previous works [55–58], we develop and adapt the theories of Flory-Stockmayer-Tanaka for thermoreversible polymerization and apply it to LIB electrolytes, where solvent molecules play an essential role in the molecular aggregation behavior, further establishing the analogy between concentrated electrolytes and polymers. In fact, this is not the first time that inspiration from polymer-based models has been used to further deepen the analogy between electrolytes and polymers. A notable example comes from Bastea [87], who developed a simple theory for the formation of chains and rings comprising of alternating cations and anions that was observed in MD simulations of a highly size asymmetric electrolyte. The inspiration for Bastea's theory for these structures came from models of wormlike surfactant micelles [95], with Bastea assuming that the monomer unit was a neutral ion pair.

The connection between Flory-Stockmayer-Tanaka theories and "patchy particle" or "spot model" systems has already been made, where a particle has a fixed number of patches or spots that can favorably interact with the patches or spots of other particles, forming thermoreversible associations [96–107]. Similarly, Stockmayer fluids, particles interacting with Lennard-Jones potentials with additional directional potentials, such as dipolar (or higher-order) interactions, have also been shown to form thermoreversible associations [84,85]. These simulation approaches are not limited to the mean-field approximation with Cayley trees, but the mean-field theories of Flory-Stockmayer-Tanaka with Cayley trees have successfully been used to understand the aggregation and gelation of patchy colloidal particles [100,101,103–105,108]. Recently, systems of oppositely charged (patchy) nanoparticles were synthesized and mixed together, forming alternating aggregates of positively and negatively charged nanoparticles [109–111].

Here, we develop a theory for a "classical" nonaqueous electrolyte—1M $LiPF_6$ dissolved in a mixture of EC and propylene carbonate (PC)—because of its importance in LIBs [1,2]. While this is used as an example here, the theory is not specifically limited to this system, and can be adapted for a wide variety of electrolytes, up to extremely high salt concentrations.

It is assumed that the cations bind with the anions and solvent molecules, but no other species bind with each other, i.e., no binding between the anion and the solvents (although this can be taken into account [55]) or between solvent molecules (which has been considered elsewhere [112]). This nonaqueous electrolyte is considered to form a polydisperse mixture of ionic clusters of rank $lmsq$,

containing l cations, m anions, s EC solvent molecules, and q PC solvent molecules, of which there are N_{lmsq} [55].

The cations can form a maximum of f_+ associations and the anions a maximum of f_- associations, referred to as their functionality. The solvent molecules are assumed to have a functionality of 1. The cations and anions are able to form extended clusters (because $f_\pm > 2$ for $LiPF_6$) [89]. However, as the concentration of the salt is relatively low and the interactions between the solvents and Li^+ cations strong, a percolating ionic network (gel) should not form at ambient conditions [55]. Therefore, for simplicity, we neglect the formation of the gel for 1M $LiPF_6$ and refer the reader to Refs. [55–58] to see how it is included.

The electrolyte is assumed to form Cayley tree clusters [55,58,113]. The cations and anions form the "backbone of the branched aggregates," and the "dangling association sites" from this backbone can either be left empty or can be decorated with the solvent molecules. Note the strong solvent-cation interactions can break apart the ionic backbone. These Cayley tree clusters have no intracluster loops, with the number of each type of bond being uniquely determined by the rank of the cluster, $lmsq$.

In Fig. 1 a schematic of some example clusters for the studied system are displayed, where the cations and anions have a functionality of 3. The cluster of rank 1300 comprises one cation and three anions, which has an overall -2 negative charge, cannot bind to any solvent molecules from the lack of open cation association sites. For 1011, the cation is bound to both solvent molecules, and there is a dangling association site that could bind to an anion or another solvent molecule to create a cluster of a larger rank. Finally, the cluster of rank 1120 is a cation-anion ion pair, where the cation is also bound to two of the s solvent molecules. These are just some examples of clusters to demonstrate the possible allowed clusters.

The assumption of Cayley tree clusters is an essential requirement of the presented theory, enabling simple analytical results, but it is important to note its potential limitations. This assumption only appears to work if there is at least one species that is disorder forming. If there are only order-forming species then the ionic aggregates that form will be crystalline in nature and have a significant number of loops [112]. For example, molten or concentrated NaCl only contains spherical, highly symmetric ions, both of which are order forming, and the resulting clusters that form are typically crystalline [88,112]. If, however, the anion is a fluorosulfonimide, the aggregates that form are no longer crystalline, but do in fact resemble Cayley trees, as we have previously shown [56–58]. Therefore, the presented theory is not applicable to all electrolytes.
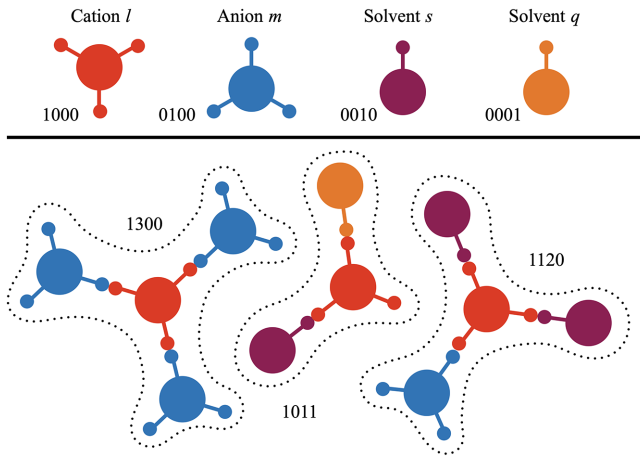
FIG. 1. Schematic showing the notation of different species. The upper panel shows cations, anions, and the two solvents, with overall quantities denoted by $+, -, x, y$, respectively, and individual species in clusters by l, m, s, q, respectively. Free cations, anions, and x and y solvents are denoted by the rank labels 1000, 0100, 0010, and 0001, respectively. In the bottom panel, example clusters are shown, where dotted lines are used to enclose each cluster.

A natural question to ask is whether this assumption works for LIB electrolytes. In "classical" nonaqueous electrolytes the salt is often $LiPF_6$, which might be thought to be an order-forming species, as both the cation and anion have high symmetry. In the context of salt-in-ionic liquids, we have shown that the Cayley tree assumption can actually be used to represent the small clusters formed in that system [58]. Moreover in Ref. [17], 4M $LiPF_6$ in EC was studied from MD simulations and experiments, and it was shown that branched, Cayley-tree-like aggregates form. In the context of next-generation electrolytes, disordered anions are often used due to their high solubility, which suggests that our theory should be applicable to these systems [114]. Moreover, the carbonate solvents are not highly symmetric species and strongly interact with the cation, which should break up any large ionic aggregates in favor of small solvation structures. Therefore, we believe the assumption of Cayley tree clusters should be justified for most LIB electrolytes.

In the presented theory, there are N_+ Li^+ cations and N_- $[PF_6]^-$ anions, and from electroneutrality in the bulk, $N_+ = N_-$. This salt is dissolved in a mixture of EC and PC, of which there are N_x and N_y, respectively. As described above and shown in Fig. 1, these species can form a polydisperse mixture of clusters of different ranks, of which there are N_{lmsq}. The theory assumes the electrolyte to be an incompressible lattice fluid (this is not an essential requirement, but is taken for convenience, and does not change the results here), with a single lattice site having the volume of a Li^+ cation, v_+ [55]. Anions occupy $\xi_- = v_-/v_+$ lattice sites, and the solvents occupy $\xi_{x/y} = v_{x/y}/v_+$ lattice

sites. Note that the volume of each species only explicitly appears in the volume fractions, and the different shapes of species are not explicitly accounted for. The total number of lattice sites is given by

$$\Omega = \sum_{lmsq}(l + \xi_- m + \xi_x s + \xi_y q)N_{lmsq}. \quad (1)$$

Dividing through by the total number of lattice sites gives

$$1 = \sum_{lmsq}(l + \xi_- m + \xi_x s + \xi_y q)c_{lmsq} = \sum_{lmsq}\phi_{lmsq}. \quad (2)$$

Here $c_{lmsq} = N_{lmsq}/\Omega$ is the dimensionless concentration of a $lmsq$ cluster (the number of $lmsq$ clusters per lattice site) and ϕ_{lmsq} is the volume fraction of clusters of rank $lmsq$. The volume fraction of each species is determined through

$$\phi_i = \sum_{lmsq}\xi_i j c_{lmsq}, \quad (3)$$

where $j = l, m, s, q$ for $i = +, -, x, y$, respectively, and $\xi_+ = 1$. The incompressibility condition can also be stated as

$$1 = \phi_+ + \phi_- + \phi_x + \phi_y. \quad (4)$$

Based on the works of Flory [59–64], Stockmayer [65–67], and Tanaka [68–76], and our previous application of this theory to concentrated electrolytes [55–58,113,115], the free energy is taken to be

$$\mathcal{F} = \sum_{lmsq}[N_{lmsq}k_B T \ln(\phi_{lmsq}) + N_{lmsq}\Delta_{lmsq}], \quad (5)$$

where the first term is the ideal entropy of each cluster of rank $lmsq$ and the second term is the free energy of forming those clusters, with Δ_{lmsq} denoting the free energy of formation for a cluster of rank $lmsq$ [55], which has three contributions,

$$\Delta_{lmsq} = \Delta_{lmsq}^{bind} + \Delta_{lmsq}^{comb} + \Delta_{lmsq}^{conf}, \quad (6)$$

where Δ_{lmsq}^{bind} is the binding energy, Δ_{lmsq}^{comb} is the combinatorial entropy, and Δ_{lmsq}^{conf} is the configurational entropy.

The binding energy of a cluster, Δ_{lmsq}^{bind}, is uniquely defined by the rank $lmsq$, owing to the assumption of Cayley tree clusters. For $l > 0$, the binding energy of a cluster is

$$\Delta_{lmsq}^{bind} = (l + m - 1)\Delta u_{+-} + s\Delta u_{+x} + q\Delta u_{+y}, \quad (7)$$

where $\Delta u_{ii'} = \Delta u_{i'i}$ is the energy of an association between i and i'. When $l = 0$, the binding energy of a cluster is 0.

Physically, the cation-anion associations are driven by their strong electrostatic interactions [55]. These associations are a representation of short-range electrostatic correlations beyond the mean-field [55–58,116–118], with Levy *et al.* [78] showing that retaining only short-range correlations in concentrated systems is sufficient to reproduce the spatial arrangements of concentrated electrolytes. The fact that we have neglected long-range electrostatic interactions *between different clusters* relies on the assumption that the majority of the electrostatic energy is incorporated in the formation of the ionic clusters (via this binding contribution). Moreover, the electrolyte is at a concentration where the activity coefficient of the salt is typically larger than 1 [2], which motivates the exclusion of further electrostatic energy terms [55], with our theory predicting such values of activity coefficients for concentrated electrolytes [55,57]. The cation-solvent associations are driven by the strong interactions between Li^+ cations and the carbonyl oxygen. It is assumed that cation-solvent interactions are the dominant contribution to the free energy of solvation, instead of, say, the Born solvation energy.

The combinatorial entropy of each cluster of rank *lmsq* is given by

$$\Delta_{lmsq}^{comb} = -k_B T \ln\{f_+^l f_-^m W_{lmsq}\}, \tag{8}$$

where

$$W_{lmsq} = \frac{(f_+l - l)! \, (f_-m - m)!}{l! \, m! \, s! \, q! \, (f_+l - l - m - s - q + 1)!}. \tag{9}$$

This entropic term was first derived by Stockmayer for applications in polymers [67]. It only depends on the number of each species in a cluster, since it is a measure of the number of ways in which a cluster of rank *lmsq* can be arranged.

The configurational entropy is associated with building the aggregate from its constituent parts on a lattice, which depends on the volume of each species. This contribution is not universal, and can depend on how "flexible" the associations are [56]. Importantly, this contribution, in the end, produces a term that depends on the number of associations in a cluster, which means that it contributes to the *entropy change of an association*, as seen in the association constant later. The binding energy and configurational entropy could, therefore, be combined into a single binding free energy, but for historical reasons, we have not described the theory in this way. We refer the reader to Ref. [56] for further details of the configurational entropy, where the temperature dependence was studied.

Establishing chemical equilibria, as shown in Ref. [55], the dimensionless concentration of a cluster of rank *lmsq*, with $l > 0$, is given by

$$c_{lmsq} = \frac{W_{lmsq}}{\Lambda_-} (\psi_l \Lambda_-)^l (\psi_m \Lambda_-)^m (\psi_s \Lambda_x)^s (\psi_q \Lambda_y)^q, \tag{10}$$

where $\psi_l = f_+ \phi_{1000}/\xi_+$ and $\psi_m = f_+ \phi_{0100}/\xi_+$ are the numbers of association sites per lattice site for free cations and free anions, respectively, and $\psi_s = \phi_{0010}/\xi_x$ and $\psi_q = \phi_{0001}/\xi_y$ are the numbers of association sites per lattice site for the free solvents x and y, respectively. The association constant between species i and cations is given by

$$\Lambda_i = e^{-\beta \Delta f_{+i}} = e^{-\beta[\Delta u_{+i} - T\Delta s_{+i}]}, \tag{11}$$

where β is inverse thermal energy and Δs_{+i} is the entropy change of an association, as determined by the configurational entropy [55,56]. Note that $i \neq +$ in these equations, as no cation-cation associations are considered. When $l = 0$ and $m = 1$ (or $m = 0$ and $l = 0$), and $s = q = 0$, Eq. (10) yields the correct limit for free anions (cations). For $l = 0$, the free volume fractions of x and y are separately defined, as $\Delta_{0010}^{bind} = \Delta_{0001}^{bind} = 0$, which is not a limit of Eq. (7).

Here, the association constants are the main parameters of the theory that need to be determined. As shown in the next section, and in our previous works [56–58], these parameters of the theory are readily determined from the ensemble average coordination numbers. Therefore, the theory does not contain any free parameters that can be arbitrarily fitted. In principle, as has been utilized in patchy particle systems, the Wertheim theory can be employed to have a parameter-free model [104–107,119–124]. This theory requires that a reference hard sphere pair correlation function and the Mayer function for the interacting species are known. As we are applying the theory to LIB electrolytes, which contain complex molecular species, we believe that using the association constants as parameters to be found by performed MD simulations, and using the theory to understand the results of these simulations in more depth, is more appropriate than making *a priori* predictions for these electrolytes.

The volume fraction of each *free* species is (usually) not a known input, however. In fact, these quantities are often what we aim to determine from the theory. To overcome this seemingly circular problem, the free volume fraction of each species can be related to the total volume fraction of that species, the number of bonds that species can make to the other species, and the probability of the associations [55]. The probability of species i being associated with species j is given by p_{ij}, the number of associations was previously defined as the functionality, and the total volume fraction of each species is known. For free cations, $\phi_{1000} = \phi_+(1 - \sum_i p_{+i})^{f_+}$, for free anions, $\phi_{0100} = \phi_-(1 - p_{-+})^{f_-}$, and for free solvent, we have $\phi_{0010} = \phi_x(1 - p_{x+})$ and $\phi_{0001} = \phi_y(1 - p_{y+})$.

The association probabilities are related through the conservation of associations and mass action laws. The conservation of associations states that

$$\psi_+ p_{+i} = \psi_i p_{i+} = \Gamma_i, \tag{12}$$

where Γ_i is the number of $+i$ associations per lattice site and $\psi_i = f_i\phi_i/\xi_i = f_i c_i$ is the number of association sites of species i per lattice site. Again, note that $i \neq +$ in these equations, which means that, for the four-component system being discussed, there are three sets of these equations. Similarly, the set of three mass action laws for the associations are generally given by

$$\Lambda_i \Gamma_i = \frac{p_{i+}p_{+i}}{(1 - \sum_{i'} p_{+i'})(1 - p_{i+})}. \qquad (13)$$

By solving the set of equations described by Eqs. (12) and (13), one can determine the association probabilities, and therefore the volume fraction of free species and the cluster distribution. For the four-component system, numerical solutions are generally required. For the assumption that there is no gel, $(f_+ - 1)(f_- - 1) > p_{+-}p_{-+}$ must hold, as this inequality determines the percolation point on a Bethe lattice [55].

In the context of polymers, Tanaka [68] introduced the mass action laws to describe the thermoreversible nature of the bonds. In electrolytes, the use of mass action laws to describe the equilibrium association has a long history, starting from Arrhenius and Bjerrum [125]. Since those early works, it has been employed countless times to model ion pairing effects [125]. Therefore, the theory presented here is an extension of these works, where we are able to account for much larger ionic aggregates in a systematic way, in addition to including solvation effects, and not requiring aggregates to be neutral.

Having outlined the basic equations, before studying the example of nonaqueous electrolytes in detail, we believe that it is prudent to summarise some intuition from limiting cases. It is suggested that the reader also goes through our general theory [55], and special cases for ionic liquids [56,113,115], water-in-salt electrolytes [57], and salt-in-ionic liquids [58], as these contain a lot of details of the ionic associations not shown here. Let us take $\Delta f_{+i} = 0$ for all i, which would correspond to $\Lambda_i = 1$. In such a case, despite the free energy of an association being zero, the association probabilities are finite, which means that there is a distribution of clusters of various ranks. This occurs because the ideal entropy of mixing and the combinatorial entropy of each cluster drives the formation of more types of clusters with more different components in them, as this increases the entropy [55,113]. We know, however, from Flory's lattice expression for the entropy of disorientation [62,63], that $\Delta s_{+i} > 0$. At low temperatures, the negative binding energies dominate, and $\Lambda_i > 1$, but at high temperatures, the entropy term dominates and $\Lambda_i \approx 0$. In this latter limit, the clusters dissociate, and we are left with only free species, with the ideal entropy of each species reducing down to the entropy of mixing of different species on a lattice [55,113].

III. CATION SOLVATION IN CLASSICAL NONAQUEOUS ELECTROLYTES

To test our theory's ability to understand cation solvation, we perform atomistic MD simulations using LAMMPS [126,127] of $LiPF_6$ in mixtures of EC and PC. For each simulation, we have 83 Li^+ cations and 83 PF_6^- anions. In addition, there are (83, 167, 250, 333, 417, 500, 583, 667, 750) EC and (750, 667, 583, 500, 417, 333, 250, 167, 83) PC solvent molecules. The initial configurations for all simulations are generated using PACKMOL [128]. An initial energy minimization is performed before equilibrating the bulk, periodic system. The production run used to analyze the associations in this system are run at 300 K in a *NVT* ensemble (the volume of the simulation box is determined from *NPT* equilibration at 1 bar) for 10 ns with a 1-fs time step.

We employ the CL&P force field for Li^+ cations and PF_6^- anions [129], with the van der Waals radius of Li^+ cations set to 1.44 Å [46]. For EC and PC, the OPLS-AA force fields are utilized [130–133], which are commonly used for simulations of these electrolytes. Long-range electrostatic interactions are computed using the particle-particle particle-mesh solver (with a cut-off length of 12 Å).

It has been shown numerous times, and as found here, that the pair correlation function (or cumulative coordination number) of Li-O (carbonyl) has a large peak (sharp increase) at about 2 Å, with a pronounced minimum (long plateau) at about 3 Å until a moderate second peak at 4–5 Å [45,46,48]. The Li-O (ether, i.e. the oxygen bonded to two carbon atoms), in contrast, has its first large peak at about 3 Å. Therefore, it is natural to define an EC and PC solvent molecule to be in the coordination shell if the Li-O (carbonyl) separation is less than 2.5 Å. However, the Li-F pair correlation function (cumulative coordination number) often has much smaller peak(s) (much steadier increase) at 3–4 Å, despite the van der Waals radius of F (in the employed MD simulation) being only slightly larger than O [45–48]. Therefore, we focus solely on the solvents in the cation coordination shell, not delving into the information about cation-anion association in this section.

Using this cut-off distance to define an association between Li^+ and EC or PC, we compute the ensemble average coordination number of Li^+ cations, $\mathcal{N}_i$, where i is one of these solvent molecules, for the various mixtures of EC and PC. The results of this simulation analysis are shown in Fig. 2, plotted as a function of the mole fraction of EC to the total mole fraction of the solvent, n_{EC}. We find that $\mathcal{N}_{EC}$ increases monotonically with n_{EC} and $\mathcal{N}_{PC}$ decreases monotonically with n_{EC}, as might be expected from an increasing proportion of EC. Their dependence on n_{EC} is nonlinear, but the sum of the solvents in the coordination shell of Li^+ remains to be approximately 4 for all n_{EC}.
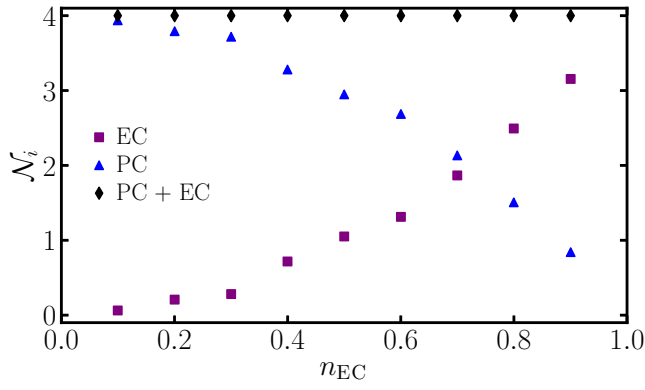
FIG. 2. Numbers of EC and PC molecules associated with Li$^+$, $\mathcal{N}_i$, as a function of the mole fraction of the EC solvent to the total mole fraction of the solvent, n_{EC}.

The composition of the first coordination shell of Li$^+$ is a quantity that is often calculated from simulations. It provides insight into the interactions in the system, and is often correlated with certain behaviors of the electrolyte, such as the conductivity or SEI-forming abilities. Moreover, within our theory, the ensemble average coordination numbers is a key quantity in determining the association probabilities, $\mathcal{N}_i = f_+ p_{+i}$, i.e., the functionality (maximum coordination number) of Li$^+$ multiplied by the probability that Li$^+$ is associated with i gives the coordination number of that species. In Fig. 2, it is clear that $f_+ = 4$. Therefore, the association probabilities of cations binding to other

species, p_{+i}, can be readily determined, and from Eq. (12), the association probabilities of species binding to Li$^+$, p_{i+}, can be found.

To progress further, we make a few simplifications. Firstly, we assume that the volumes of EC and PC molecules are the same, and, therefore, the volume fraction of LiPF$_6$ is constant (note that this is not a necessary assumption, and does not change the results significantly, but it is done for convenience). Secondly, the total Li$^+$ coordination number is consistently 4, which means that Li$^+$ has practically no "dangling bonds" because the interactions between Li$^+$ and the solvents are so energetically favorable. This means that the probability of Li$^+$ binding to solvents is equal to unity, $1 = p_{+x} + p_{+y}$, which we refer to as the "sticky cation" approximation [57]. From inspecting Eq. (13), with only solvent molecules included in the summation over i', it should be clear that there is singular behavior because the probability of an open cation site, which is 0 in the sticky cation approximation, sits in the denominator of the equation. This singular behavior needs to be removed from the system of equations. By dividing the mass action laws between Li$^+$ and the two different solvents, we arrive at

$$\frac{\Lambda_x}{\Lambda_y} = \tilde{\Lambda} = \frac{p_{x+}(1 - p_{y+})}{p_{y+}(1 - p_{x+})}, \tag{14}$$

which is no longer singular. Using this equation, in addition to $1 = p_{+x} + p_{+y}$, permits analytical solutions for the association probabilities:

$$\psi_+ p_{+x} = \psi_x p_{x+} = \frac{\psi_y - \psi_+ + \tilde{\Lambda}(\psi_+ + \psi_x)}{2(\tilde{\Lambda} - 1)} - \frac{\sqrt{4\psi_y \psi_+(\tilde{\Lambda} - 1) + [\tilde{\Lambda}(\psi_x - \psi_+) + \psi_+ + \psi_y]^2}}{2(\tilde{\Lambda} - 1)}, \tag{15}$$

$$\psi_+ p_{+y} = \psi_y p_{y+} = \frac{\psi_y + \psi_+ + \tilde{\Lambda}(\psi_x - \psi_+)}{2(1 - \tilde{\Lambda})} - \frac{\sqrt{4\psi_y \psi_+(\tilde{\Lambda} - 1) + [\tilde{\Lambda}(\psi_x - \psi_+) + \psi_+ + \psi_y]^2}}{2(1 - \tilde{\Lambda})}. \tag{16}$$

When $\tilde{\Lambda} > 1$, the associations between Li$^+$ and EC are favored over Li$^+$ and PC ($\Lambda_x > \Lambda_y$), and when $\tilde{\Lambda} < 1$, the associations between Li$^+$ and PC are favored over Li$^+$ and EC ($\Lambda_y > \Lambda_x$). The other factor in determining the association probabilities is the amount of each species. Therefore, in the sticky cation approximation, we only have a single parameter of the theory that needs to be determined from the MD simulations.

In Fig. 3 we show the probabilities computed from the values of $\mathcal{N}_i/f_+$ obtained from our MD simulations as a function of n_{EC}. Using these probabilities, we can

compute $\tilde{\Lambda}$ from Eq. (14) at each n_{EC} and take the average of the obtained values. We find $\tilde{\Lambda} = 0.135$, which indicates that PC has more favorable associations with Li$^+$ than EC (which can also be seen in Fig. 3 from $p_{y+} > p_{x+}$ for all n_{EC}). Now that $\tilde{\Lambda}$ has been determined, and there are no other free parameters of the theory, Eqs. (15) and (16) can be used to predict the association probabilities for any value of the variable n_{EC}. In Fig. 3 we show that these probabilities match the simulated values extremely well. Therefore, our simple, analytical theory can allow us to naturally understand the solvation structure competition

FIG. 4. Coordination probability of s EC molecules, c_s/ϕ_+, as a function of n_{EC}. The same set of parameters used in Fig. 3 is used for the lines.
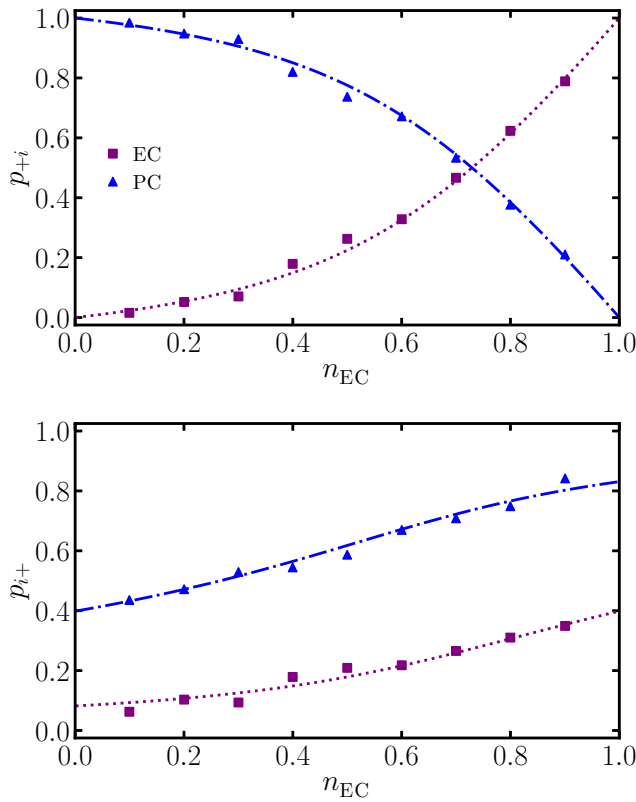

FIG. 3. Association probabilities as a function of the mole fraction of EC relative to the mole fraction of the solvent. Symbols are values directly extracted from simulations. Lines are values calculated from Eqs. (15) and (16) using $f_+ = 4$, $f_{x/y} = 1$ $\tilde{\Lambda} = 0.135$, $\phi_\pm = 0.093$, and $\xi_{x/y} = 28.75$.

of concentrated Li$^+$ electrolytes. Having understood the association probabilities, we can now turn to the distributions of solvation structures.

In Fig. 4 we display the probability of s EC solvent molecules in the coordination shell of the Li$^+$ from the simulations for $s = 0, \ldots, 4$ as a function of n_{EC}. For $s = 0$, i.e., Li$^+$ only being solvated by PC, the probability of this solvation structure is initially close to 1, and it monotonically decreases with increasing n_{EC}. However, $s = 1, 2, 3$, i.e., mixed EC and PC solvation structures, all have a nonmonotonic dependence on n_{EC}, where they go through a maximum at intermediate n_{EC}. Finally, $s = 4$, i.e., only EC associated with Li$^+$, monotonically increases with n_{EC}, where it is the largest component in the coordination shell at the largest n_{EC}.

To investigate the solvation distribution from the theory, the singular behavior needs to be removed from Eq. (10) in the sticky cation approximation. Using $1 = p_{+x} + p_{+y}$, $f_+ = s + q$, and Eq. (14), we can arrive at

$$\frac{c_s}{\phi_+} = \frac{f_+!}{s!\,(f_+ - s)!} p_{+x}^s (1 - p_{+x})^{f_+ - s}, \qquad (17)$$
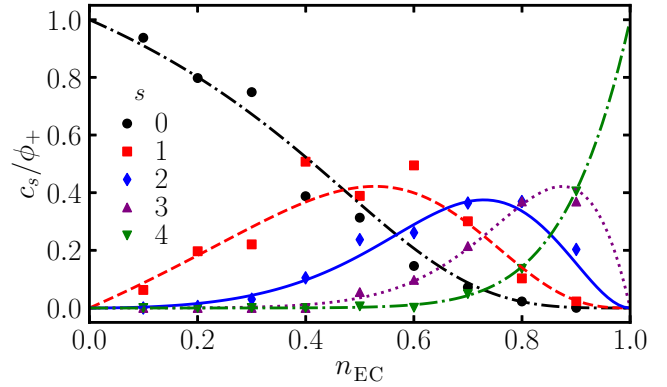
which is the probability of s EC solvent molecules in the coordination shell of the Li$^+$, with c_s being used as a shorthand for c_{10sq}. An equivalent expression for the probability of q PC solvent molecules in the coordination shell of the Li$^+$, c_p, can be derived. Equation (17) is clearly the number of ways of arranging a solvation shell with s EC and q PC solvent molecules, multiplied by the probability that s solvent molecules are bound to the Li$^+$ and the probability that the remaining $f_+ - s$ PC molecules are bound to Li$^+$, i.e., it is simply a binomial distribution of the two solvent molecules.

In Fig. 4 we also plot the probability of s EC molecules in the coordination shell of Li$^+$ from the theory, using the value of $\tilde{\Lambda}$ extracted from the simulations. Overall, we find good agreement between the theory and simulation. The theory allows us to understand this dependence of c_s/ϕ_+ on n_{EC}. For $s = 0$, Eq. (17) reduces to $p_{+y}^{f_+}$, and for $s = f_+ = 4$, we arrive at $p_{+x}^{f_+}$, which are clearly the probabilities of f_+ PC and EC molecules binding to the Li$^+$ cation, respectively. As can be understood from Fig. 3, these functions, $p_{+y}^{f_+}$ and $p_{+x}^{f_+}$, are monotonically decreasing and monotonically increasing, respectively. For all values of s between these limits, both p_{+x} and $1 - p_{+x}$ occur in the expressions, which requires that c_s goes to zero at the limits of n_{EC}, and that a maximum occurs between these limits. If $\tilde{\Lambda} = 1$, the $s = 2$ case would peak at $n_{EC} = 1/2$, but because $\tilde{\Lambda} < 1$, the peak occurs at $n_{EC} > 1/2$ as clusters with PC are favored and larger concentrations of EC are required to reach this point. This demonstrates that the binomial distribution is skewed based on the relative interactions of the solvents with Li$^+$.

A. Experimental comparison

In Ref. [19] mass spectra of 1M LiPF$_6$ in mixtures of nonaqueous solvents were measured. As the electrolyte is vaporized and ionized from the liquid state, it is thought
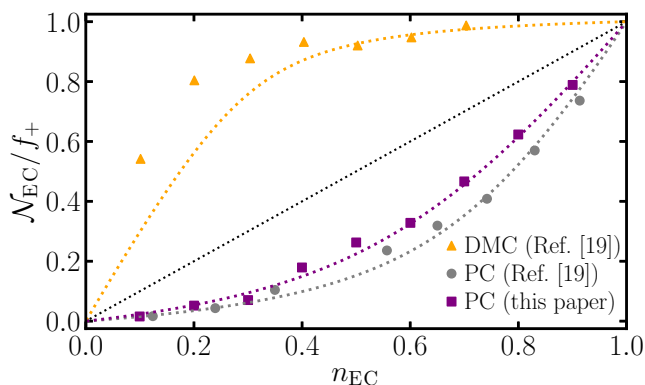
FIG. 5. Fraction of EC molecules in the coordination shell of Li^+ as a function of the mole fraction of EC relative to the mole fraction of the solvent, n_{EC}. For EC-PC mixtures, the values from Ref. [19] and our simulations from the previous section are shown. The EC-DMC mixtures from Ref. [19] are also displayed. The values of the parameters for the theory are computed from the association probabilities $p_{+x} = \mathcal{N}_{EC}/f_+$. For the experimental values, we take $f_+ = 3$ as it fits the values significantly better, and we find that $\tilde{\Lambda} = 0.0978$ for EC-PC mixtures and $\tilde{\Lambda} = 26.7$ for EC-DMC mixtures. All other values are kept the same as those in Fig. 3.

that most of the strong associations stay in tact, and, therefore, the mass spectrum can provide information of the distribution of solvation structures in the liquid electrolyte. Therefore, the solvation structure of cations is a physical observable that we can directly compare our theory against. In Fig. 5 we reproduce the values of Ref. [19] for the fraction of EC in the solvation shell, i.e., $\mathcal{N}_{EC}/f_+$, for EC-PC and EC-DMC mixtures, as a function of the mole fraction of EC relative to the mole fraction of total solvent. In addition, we reproduce the values simulated from the previous section. As we know $p_{+x} = \mathcal{N}_{EC}/f_+$ from experiments, assuming the sticky cation approximation, we are able to calculate values of $\tilde{\Lambda}$ for the experiments, and compare our theory against these values.

For EC-PC mixtures, the values of $\mathcal{N}_{EC}/f_+$ from simulations and experiments are quite similar. In the experiments, it was noted that up to only three coordinating solvent molecules were found. The discrepancy between simulations and experiments as to whether a maximum of three or four solvent molecules can coordinate lithium in these carbonate blends was discussed in Ref. [19] and thought to be an attribute of the electrospray ionization technique only retaining the most tightly bound species. Therefore, for the experimental data, we use $f_+ = 3$, finding that $f_+ = 4$ fitted the curves worse than $f_+ = 3$. Based on this functionality, we calculated $\tilde{\Lambda} = 0.0978$ for the experiments, which is similar to the value obtained from the simulations. This value of $\tilde{\Lambda}$ indicates that the PC-Li^+ associations are more favorable than the EC-Li^+ associations, which is evident

from the curves being below the diagonal dotted line that corresponds to $\tilde{\Lambda} = 1$.

On the other hand, for the EC-DMC mixtures, the EC-Li^+ associations are favored over the DMC-Li^+ associations, and so $\mathcal{N}_{EC}/f_+$ resides above the diagonal. The value of $\tilde{\Lambda} = 26.7$ extracted from the experimental data is now larger than 1, demonstrating the more favorable EC-Li^+ associations. Therefore, the value of $\tilde{\Lambda}$ is a clear, physical parameter that describes the competition between the solvation structure of Li^+ electrolytes. Again, $f_+ = 3$ did a better job at reproducing the data than $f_+ = 4$.

There are many examples of simulations that show similar trends to those reported in Ref. [19]. While there can be some differences in the reported experimental or predicted values from simulations, with and without associations between cations and anions, we wish to stress that our theory should be able to capture the behavior of all these systems, provided the assumptions of the theory are valid. What changes is the exact volume fractions of species, association constants and functionalities.

IV. BEYOND CLASSICAL NONAQUEOUS ELECTROLYTES

In previous sections, we focused on cation solvation in common nonaqueous electrolytes that are studied primarily for use in commercial LIBs. We chose this electrolyte because it has been extensively studied, and the coordination structure is qualitatively agreed upon. While these electrolytes are commonly and successfully used in commercial LIBs, moderately concentrated carbonate blend electrolytes generally do not perform well in many next-generation battery technologies [4–8]. For such applications, there are many emerging classes of electrolytes currently being explored in the literature, for which our developed theory can be adapted [4–8,89,134].

In this section, we utilize our theory to understand some "design principles" of several classes of next-generation electrolytes currently being investigated. Note we have only picked a few examples to discuss here to demonstrate the theory's ability, with an exhaustive comparison being left for future work. We mainly focus on "toy models" of the theory for these electrolytes, details of which are shown in Appendix A–C, and we do not perform simulations to back up these findings, but hope that these results inspire further investigation of these systems. For brevity, we will not review in detail why these next-generation electrolytes are of interest or their exact chemistries, but refer the reader to where this information can be found.

A. Localized high-concentration electrolytes

The design of LHCEs—the reader is referred to Ref. [28] for a review—starts from finding a promising highly concentrated electrolyte (HCE), typically just a salt dissolved in a solvent that solvates the cation strongly. This

HCE is then diluted with a solvent that does not solvate the cation, known as the diluent, in an attempt to preserve the coordination structure of the cation (see the Introduction for why this is important). Therefore, the lithium coordination shell—likely invaded by anions—resembles one that could typically be obtained at only high salt concentrations in two-component mixtures. From the perspective of the lithium ions in solution, the electrolyte is "locally" concentrated.

From our toy model, shown in Appendix A, we find that the design principle of LHCEs is supported by our theory, under certain approximations. In the sticky cation approximation, the addition of a diluent, which does not interact with any other species, leaves the coordination shell of the cations unchanged, despite the dilution effect. If the sticky cation approximation is not employed, the predictions of the theory sensitively depend on the assumed association constants, and, therefore, we do not make any predictions for this case. Using our theory, it should be possible to reveal the necessary components to include in a model that accurately describes these promising electrolytes.

B. High entropy electrolytes

Within the chemistries of LHCEs, it has been proposed that, by adding more types of solvents, without changing the concentration of salt and the solvation enthalpy, the average cluster size decreases while retaining roughly the same number of anions in the coordination shell of Li$^+$ [135]. This is thought to occur because of the increased entropy of mixing, similar to high entropy alloys, which is why this system has been referred to as a high entropy electrolyte (HEE) [135]. This HEE has been reported to have significantly better transport properties, without diminishing the stability of the electrolyte [135].

The toy model we utilize to investigate this system is shown in Appendix B. We find that our theory does not support the design principle of this HEE. More types of solvent, which interact identically with the cation, leave the average cation-anion cluster size unaltered. In Appendix B, we have given some possible explanations as to why this could be, but reserve making final, physical conclusions until a detailed comparison can be made between our theory and simulations of these electrolytes. We believe that it is essential to perform this comparison to understand the origin of the electrolytes' promising transport properties [135].

In addition to Ref. [135], there are now further examples of electrolytes that claim to be high entropy [136–138]. In Appendix B we further discuss these examples, although we do not specifically develop theories for these cases. We also provide a general discussion of the ideas of high entropy alloys and oxides [139] and what this could mean for electrolytes, and refer the reader to reviews on the role of entropy in self-organized structures [140–142], which

will provide insight into the role of entropy in concentrated electrolytes, and especially high entropy electrolytes.

C. Chelating agents

Solvents that can bind to cations from multiple points, i.e., multidentate ligands, have been proposed to be beneficial in reversing the negative transference numbers of salt-in-ionic liquids [58,143,144]. A limiting case of such electrolytes is when the solvent completely encapsulates the cation, preventing it from binding to any other species, be it anions or other solvent molecules. The "design principle" of the addition of encapsulating chelating agents is to break up the cation-anion associations and preventing multiple anions from binding strongly to the cations [145]. Here we develop an approach to include these multidentate, encapsulating solvents, to see if this principle is supported by our theory.

Our developed theory extension for this type of solvent, shown in Appendix C, yields predictions that are consistent with those of Ref. [145], i.e., dissociation of larger clusters upon the addition of a chelating agent which encapsulates the cation. Therefore, the design principle of adding chelating agents that encapsulate the cations is supported by our simple theory. Further work should compare how the cluster distribution is altered by the presence of these chelating agents in detail.

D. Soft solvents

While mixtures of carbonate solvents have been used in commercial LIB electrolytes for a while, these electrolytes do not perform optimally, and it is known that the solvents are strongly bound to Li$^+$. Such solvents have high binding energies and dielectric constants, which ensures the solubility of salts such as LiPF$_6$, but causes slow desolvation dynamics, amongst other issues. To overcome this, and related issues, it has been suggested to instead employ "soft solvents" that have a fairly low binding energy, but still a modest dielectric constant, in order to reduce the strength of the cation-anion interaction [134]. With these soft solvents, highly dissociating salts are required, but these mixtures have highly promising transport, interfacial and interphasial properties, and temperature operating ranges [134].

While we do not need to specifically develop a toy model for soft solvents, as it already falls within the theory presented, we would like to highlight a few points. As we have shown here, the association constants are the physical parameters that describe the association strength, which combines information about the association energy and dielectric constant, as well as the entropy of association [56]. By plotting where different LIB electrolytes are on a graph of Λ_{+-} as a function of Λ_{+x}, the competition of anion and solvent associations for different LIB electrolytes can be characterized. For example, we expect soft

solvent systems to have relatively small Λ_{+-} and Λ_{+x}, but commercial LIB electrolytes have a large Λ_{+x} and small Λ_{+-}. The magnitudes of the association constants are directly linked to the lifetime of the associations, and therefore the timescales of association and disassociation [97,101,146–149].

V. CONCLUSIONS

In summary, we have developed a theory for the solvation structure and ionic aggregation of nonaqueous electrolytes. We have tested this theory against molecular dynamics simulations of a "classical" nonaqueous electrolyte, 1M LiPF$_6$, in mixtures of carbonates. Overall, we found excellent agreement between our theory and the classical molecular dynamics simulations, and our theory also worked well in comparison to already published experimental results for the competition between EC and PC in the coordination shell of Li$^+$. Confident in the theory, we investigated nonaqueous electrolytes of interest in the next generation of LIBs. Overall, it is hoped that this theory will provide a framework for understanding the solvation shell of electrolytes in a more systematic way, and aid the design of next-generation chemistries.

While we have focused on the solvation structure of the cations here, which is known to be crucial in understanding the properties of LIB electrolytes, our theory can be directly used to calculate physiochemical properties of interest, which can quantify the connection between solvation structure and properties of interest. For example, we have developed a consistent treatment of ionic transport based on vehicular motion of species, which could be used to understand conductivity and transference numbers of different mixtures [56,58]; we can calculate activity coefficients from our theory [57], which can provide indications of whether the electrolyte is expected to form a stable SEI; and we recently developed the theory to predict the composition of electrolytes at charged interfaces [113,115], where desolvation of cations could be a result of the breakdown of the cluster distribution at an interface. In our experience, the theory has qualitatively worked for all of these applications, but quantitatively it does best for transference numbers and activity coefficients, with conductivity and double layer properties being more difficult to predict. We believe that the value of the theory is its physical transparency that allows a conceptual understanding in these LIB electrolytes.

Looking forward, our theory could be developed to understand the kinetics of SEI formation [150–152] in more detail with explicit account of the solvation shell, and electron transfer reactions of solvated cations at interfaces [153,154], where the reorganization energy could be linked to the free energy of forming those clusters. Here we focused on nonaqueous electrolytes, and previously we have studied ionic liquids [56], water-in-salt electrolytes [57] and salt-in-ionic liquids [58], but the theory is quite general, and could be applied to a wide variety of electrolytes, from high concentration to low concentration (provided long-range electrostatics are introduced [55]), for various temperatures [56] and for various types of solvent (aqueous and nonaqueous) and salt compositions, provided Cayley tree clusters are formed.

The theory we present here is simple, but we believe that it acts as a good starting point for further work. One of the main limiting assumptions of the theory is the formation of Cayley trees, with only two species that can form the backbone of a percolating network. In reality, this assumption only holds for specific electrolytes. Fortunately, LIB electrolytes mainly appear to fall within this category, but certain high entropy electrolytes, or electrolytes with order forming species, break our assumptions. Therefore, we believe that it is important to further develop theories [123,155,156] and perform simulations beyond the assumptions here [88,90–93].

APPENDIX A: LOCALIZED HIGH-CONCENTRATION ELECTROLYTE

Our toy model for LHCE first fixes a relative composition of HCE with cations, and anions and solvent molecules that bind to the cations. All of these components are then equally diluted. This additional cosolvent that dilutes the HCE, making the LHCE, is introduced as any other solvent in the theory, but with an association constant of 0. Therefore, no additional mass action or conservation of association equations needs to be introduced, and all that changes is the new volume fractions of the cation, anion, and solvent that are given by $\phi_i^d = \phi_i(1 - \phi_d)$, where ϕ_d is the volume fraction of the diluent and ϕ_i^d is the new volume fraction of each diluted species.

Let us first look at the predictions from the "sticky cation" approximation. For the anion and a single solvent in the coordination shell of the cation, we have

$$\frac{\Lambda_-}{\Lambda_x} = \tilde{\Lambda} = \frac{p_{-+}(1 - p_{x+})}{p_{x+}(1 - p_{-+})}, \tag{A1}$$

which together with $1 = p_{+-} + p_{+x}$ permits analytical solutions for the association probabilities:

$$\psi_+ p_{+-} = \psi_- p_{-+} = \frac{\psi_x - \psi_+ + \tilde{\Lambda}(\psi_+ + \psi_-)}{2(\tilde{\Lambda} - 1)} - \frac{\sqrt{4\psi_x \psi_+ (\tilde{\Lambda} - 1) + [\tilde{\Lambda}(\psi_- - \psi_+) + \psi_+ + \psi_x]^2}}{2(\tilde{\Lambda} - 1)}, \tag{A2}$$

$$\psi_+ p_{+x} = \psi_x p_{x+} = \frac{\psi_x + \psi_+ + \tilde{\Lambda}(\psi_- - \psi_+)}{2(1 - \tilde{\Lambda})} - \frac{\sqrt{4\psi_x \psi_+ (\tilde{\Lambda} - 1) + [\tilde{\Lambda}(\psi_- - \psi_+) + \psi_+ + \psi_x]^2}}{2(1 - \tilde{\Lambda})}. \tag{A3}$$

In the above equations, the replacement of ψ_i for ψ_i^d can be made. It is clear that the factor $(1 - \phi_d)$ that multiplies all original volume fractions of species completely cancels from the expressions. Therefore, for a fixed $\tilde{\Lambda}$, within the sticky cation approximation, there is no effect from the diluent on the association probabilities, and the coordination shell of the cation remains identical to the HCE it is derived from.

To further understand LHCEs, let us investigate a mass action law where $1 > \sum_{i'} p_{+i'}$, i.e., not the sticky cation approximation. If the association probabilities are to remain unchanged by the addition of the diluent then $\Lambda_i \Gamma_i$ must remain unchanged. The value of Γ_i should, however, decrease with increasing volume fraction of the diluent. Therefore, there must be a corresponding increase in Λ_i to compensate, to keep $\Lambda_i \Gamma_i$ constant. When taking the ratio of the association constants in the sticky cation approximation, this increase in the Λ_i is hidden.

It is known that the coordination structure of the cation does change [28], which is perhaps not surprising, as in reality $\tilde{\Lambda}$ (or the Λ_i) will not correspondingly increase. It is thought that the diluent can interact with the solvent molecules as well as change the dielectric constant of the mixture, resulting in an increase of anion molecules in the cation coordination shell [28].

One can account for short-range interactions between the solvent and diluent through a regular solution interaction, similar to how we treated the ionic liquid cations in salt-in-ionic liquids [58]. This will tend to remove the solvent molecules from the solvation shell of Li$^+$, which should exponentially depend on the volume fraction of the diluent. By computing the concentration dependence of the association constant on the diluent volume fraction, it should be clear exactly how the interaction appears.

On the other hand, the diluent changes the dielectric constant of the mixture and the concentration of associating species that, presumably, alters the association constants in a different way. Predicting the exact changes that will happen is difficult, but by performing simulations of specific LHCEs and extracting the association probabilities and constants, one can further understand the simulations from the developed theory.

APPENDIX B: HIGH ENTROPY ELECTROLYTES

Our toy model for the HEEs of Ref. [135] assumes a fixed volume fraction of salt, with the cation-anion association constant fixed. The total volume fraction of the solvent also remains constant, but its composition can be divided up between multiple different solvents. For now, let us assume that these solvents can solvate the cation, and that there is no diluent present. These solvents are essentially only different in the sense that they are labeled differently, as we take their volumes ($\xi_1 = \xi_{2,2} = \xi_{2,1}$) and association constants with the cations to be identical ($\Lambda_1 = \Lambda_{2,2} = \Lambda_{2,1}$), where index 1 is used for the single solvent, and indexes 2, 1 and 2, 2 are used to denote the solvents in the system with two solvents. Therefore, the only difference between a system with one solvent (with ϕ_1) and another with two solvents (with $\phi_1 = \phi_{2,1} + \phi_{2,2}$) is the entropy of the systems. We include the entropy of mixing, configurational entropy, and conformational entropy of clusters, as shown in Sec. II of the main text.

Furthermore, let us first focus on a limiting case where the solvent-cation interactions are extremely strong, $\Lambda_i \gg 1$, with the cation-anion association constant much smaller, $\Lambda_i \gg \Lambda_-$, and when there are more cation association sites than solvent association sites, i.e., $c_+ f_+ > \sum_i c_i$. In such a case, the probability of the solvent associating with the cation is, of course, $p_{i+} = 1$. From the conservation of associations, the cation association probabilities to the solvents are $p_{+i} = \psi_i / \psi_+$. For the single-solvent system, we have $p_{+1} = \psi_1 / \psi_+$, and for the two-solvent system, we have $p_{+2,2} = \psi_{2,2} / \psi_+$ and $p_{+2,1} = \psi_{2,1} / \psi_+$. Clearly, then, we find that the total probability of a cation being associated with a solvent molecule remains the same between one and two types of solvent molecules, with the relationship $p_{+1} = p_{+2,1} + p_{+2,2}$ holding. In fact, as we found from numerically solving the mass action laws, this relationship holds irrespective of the employed association constants (provided the solvent-cation association constants are the same) and volume fractions of species.

With the previously derived results for p_{+i}, it is clear that the cation-anion mass action law, as generally given by

$$\Lambda_- \Gamma_- = \frac{p_{+-} p_{-+}}{(1 - p_{+-} - \sum_i p_{+i})(1 - p_{-+})}, \tag{B1}$$

remains unchanged by the presence of more types of solvents that interact with the cation identically. Unsurprisingly, then, the cation-anion probabilities remain the same, independent of the number of "different" solvents in the system. As the cations and anions form the backbone of the "alternating ionic copolymer" of Cayley-tree-like

clusters, if their probabilities of association do not change then the cation-anion cluster distribution, after summing out the solvent indexes, does not change. Moreover, the percolation threshold is determined by $(f_+ - 1)(f_- - 1) = p_{+-}p_{-+}$ for Cayley tree clusters, which also cannot change from adding more types of "different" solvents.

We explicitly show how the cluster distribution is not effected by the number of different solvents, again by considering the cases of one solvent and two solvents. For clarity of notation, we take $\Lambda = \Lambda_1 = \Lambda_{2,2} = \Lambda_{2,1}$. The cluster distribution for one solvent is generally given by

$$c_{lms} = \frac{W_{lms}}{\Lambda_-}(\psi_l \Lambda_-)^l (\psi_m \Lambda_-)^m (\psi_s \Lambda)^s. \quad (B2)$$

Let us assume that there is some combination of l and m such that there are only n cation association sites remaining. Therefore, we arrive at

$$\frac{c_{ns}}{c_n} = \frac{n!}{s!\,(n-s)!}(\psi_s \Lambda)^s, \quad (B3)$$

where the shorthand c_n is used for the cluster distribution of this cation-anion combination with n cation association sites remaining.

Similarly, the cluster distribution for two solvents is

$$c_{lmpq} = \frac{W_{lmpq}}{\Lambda_-}(\psi_l \Lambda_-)^l (\psi_m \Lambda_-)^m (\psi_p \Lambda)^p (\psi_q \Lambda)^q, \quad (B4)$$

and again considering n cation association sites being free, we have

$$\frac{c_{npq}}{c_n} = \frac{n!}{p!\,q!\,(n-p-q)!}(\psi_p \Lambda)^p (\psi_q \Lambda)^q. \quad (B5)$$

Given that the probabilities p_{i+} are not altered, and that the volume fraction of the solvent remains constant, it is clear that the following relationship holds for any s:

$$c_{ns} = \sum_{pq}^{s=p+q} c_{npq}. \quad (B6)$$

This is simply a binomial distribution of the two solvents in place of the single solvent, which does not alter how much solvent is associated with the clusters. While we have shown this for only two solvents here, it is expected that it generalizes to any number of solvents, with there being a multinomial instead of a binomial distribution.

Another example of a HEE could be from keeping the solvating solvents the same, but increasing the number of diluent solvents. From the previous section on LHCEs, as these diluents do not associate with the cation ($\Lambda = 0$), if they interact with the solvents identically (say through the same regular solution term χ), and have the same dielectric

constant, it is clear that more diluents should not alter the cation-anion association probabilities or the cation-solvent probabilities.

We can conclude then that the design principle of HEEs is not supported by our theory. We find that, for solvents that interact with the cation (and other solvents) identically, more types of solvents do not alter the cation-anion cluster distribution or percolation point, provided the cation-anion association constant is fixed.

These electrolytes are, however, advantageous for some reason, as their transport properties clearly show [135]. There could be two possible reasons why our theory does not support the assumed principle of this HEE. One possibility is that the fundamental assumptions of our theory (Cayley tree clusters, neglecting long-range electrostatics, the free energy of formation of a cluster, monodentate solvent molecules, etc.) are flawed in some way and cannot be applied to this HEE. The other possibility is that, while the solvents interact with the cation in a similar way, they are never *exactly* the same, and the changes to the properties of the electrolyte occur because of the slight differences in their association constants (or functionalities, volumes, etc.), instead of the proposed increase in the entropy of mixing. Only by a detailed comparison between the proposed toy model and atomistic simulations can the origin of the discrepancy be unveiled. In Appendix D, a method for systematically performing such comparisons of solvation and aggregation behavior is outlined.

In addition to Ref. [135], there are now further examples of "high entropy electrolytes." Yang *et al.* [138] combined LiCl and ZnCl$_2$ in water at various compositions, and found a 2:1 ratio with nine water molecules per formula unit yielded an optimal transport and stability compromise, performing significantly better than water-in-salt [157]. This occurs because the Li$^+$ coordination shell is mostly water, with Zn^{2+} being consistently coordinated by 4Cl$^-$ anions. The authors argued that this electrolyte was distinct from "water-in-bi-salt," because of the observed properties being distinct from previous water-in-bi-salt systems [158,159]. We, however, disagree with this conclusion and believe that the difference in the behavior occurs from differences in the interactions of the cations with water and chloride [138]. In previous water-in-bi-salt systems [158], there was typically only one strongly coordinating cation, with the other being a weakly interacting ionic liquid cation. This meant that the water and anion are in competition for the coordination sites of the cation. In Ref. [138], however, two strongly coordinating cations are used, and their preferential solvation behavior and 2:1 ratio assists Li$^+$ being solvated by water and Zn^{2+} by Cl$^-$. We believe that this system can be modeled by a combined and modified version of our theories for salt-in-ionic liquids [58] and water-in-salt electrolytes [57].

Wang *et al.* [137] investigated the liquid-solid phase behavior of mixtures of Li$^+$ salts with numerous anions.

Overall, it was found that, when five anions are present, there is a suppression of precipitation. It was claimed that this occurs due to the larger number of different anions in the coordination shell of Li$^+$. While we cannot explicitly develop a theory for this example, as there are many species with $f_i > 1$, this conclusion would very naturally follow from our theory if this limitation was overcome, provided Li$^+$ interacts with all anions with a similar free energy of association. Moreover, linking the suppression of precipitation from disordered coordination environments is conceptually similar to engineering the phase behavior in high entropy alloys and oxides. We believe that in this electrolyte, the ordered clusters of two species should be suppressed in favor of disordered, branched aggregates with many different species. In addition, it was found that transport properties were improved, but no link was suggested to the exact coordination environment, other than it being disordered. Overall, we believe that extensions of our theory will support the conclusions made for this electrolyte being high entropy, but further analysis of the simulation results will be required to completely understand this promising system.

In high entropy alloys and high entropy oxides, the crucial requirements are that a large number of relatively similar components exist, often at least five, and that the difference in how these species interact with other species is small, which motivates neglecting interaction terms and only retaining the entropy of mixing [139]. We believe that the requirements that there are at least five components of cations or anions or solvents or diluents and that these components interact similarly with other components are the conditions for an electrolyte to be high entropy. In addition, in LIB electrolytes, presumably only one active cation is desired, and diluents do not interact strongly with other species, which means that only multiple anions or solvents are potentially promising avenues. Kim *et al.* [135] showed that the solvents had a similar solvation enthalpy, but only three different coordinating solvents were considered, which might not conceptually be thought of as high entropy (at least according to high entropy alloys and oxides [139], but in electrolytes the number of components that make it high entropy could be smaller than that of alloys and oxides). In Ref. [138] again only two cations were considered, and they interacted with water and the chloride ions very differently, which means that both conditions are not satisfied. In Ref. [137], five different anions were investigated, but it was not explicitly shown that they have a similar interaction strength with the other components, although their reported clusters suggest that they could be similar. Thus, Ref. [137] should satisfy both of the requirements for a high entropy electrolyte.

It is also crucial to note that the role of entropy in self-assembling systems is very different to, and significantly more complicated than, high entropy alloys and oxides. In high entropy alloys and oxides there is essentially only the entropy of mixing. In the theory presented here, which builds on previous works on self-assembled systems, there is the entropy of mixing all clusters, but also the combinatorial and configurational entropies of the clusters. For free species, the combinatorial entropy is 0, but when there are large species with many ways of arranging them, the entropy substantially increases. Therefore, entropy actually drives the formation of large clusters. We refer the reader to Refs. [140–142] for further discussion of these concepts in self-assembled systems, as these ideas will be useful to understand high entropy electrolytes.

APPENDIX C: CHELATING AGENTS

In this section, we outline modifications to the theory that allow chelating agents to be included. This is the starting point for the inclusion of solvent molecules that are multidentate, but that do not completely encapsulate a cation. We do not solve this problem in its full complexity, but simply outline the principles, leaving an in-depth analysis for future work.

The chemical equilibrium between free species and the higher ranking clusters determines the cluster distribution, and the free cation concentration is one of the key variables in this balance. If there are anions and solvents, and another solvent that can encapsulate the cation, the free cation concentration is given by the probability of not being bound to the anions and/or solvents and the encapsulating solvent, as seen through

$$\phi_{100} = \phi_+ p_f p_c, \tag{C1}$$

where the probability of not being bound to any anions or singly solvating molecules is given by

$$p_f = \left(1 - \sum_i p_{+i}\right)^{f_+}, \tag{C2}$$

and the probability of not being encapsulated by one of the chelating agents is given by

$$p_c = 1 - p_{+c}. \tag{C3}$$

Crucially, the cation behaves as if it has a functionality of 1 when binding to the encapsulating solvent molecule.

The free cation concentration can be recast into a more familiar form

$$\phi_{100} = \phi_+^c p_c, \tag{C4}$$

where there is a renormalized volume fraction of cations that are not bound to anions and/or solvent,

$$\phi_+^c = \phi_+ \left(1 - \sum_i p_{+i}\right)^{f_+}. \tag{C5}$$

Equivalently, the free cation volume fraction can be written as

$$\phi_{100} = \phi_+^i p_f \tag{C6}$$

with a renormalized cation volume fraction without any associations to the encapsulating solvent of

$$\phi_+^i = \phi_+(1 - p_{+c}). \tag{C7}$$

The important point to note is that the renormalized volume fractions of cations can be treated as unknowns that need to be found.

From these observations, a set of modified mass action laws and conservation of associations can be stated. For the encapsulating solvent, we have, for the mass action law,

$$\Lambda_c \Gamma_c = \frac{p_{+c} p_{c+}}{(1 - p_{+c})(1 - p_{c+})}, \tag{C8}$$

and for the conservation of associations,

$$\Gamma_c = \psi_+^c p_{+c} = \psi_c p_{c+}, \tag{C9}$$

where $\psi_+^c = \phi_+^c / \xi_+ = \phi_+(1 - \sum_i p_{+i})^{f_+} / \xi_+$ with $i \neq c$.

The mass action laws for the cation associations to the anions and solvents are similar to the case before, i.e.,

$$\Lambda_i \Gamma_i^c = \frac{p_{+i} p_{i+}}{(1 - \sum_i p_{+i})(1 - p_{i+})} \tag{C10}$$

with conservation of associations

$$\Gamma_i^c = \psi_+^i p_{+i} = \psi_i p_{i+}, \tag{C11}$$

where $\psi_+^i = \phi_+^i p_{i+} / \xi_+ = \phi_+(1 - p_{+c}) / \xi_+$.

Now, Eqs. (C8)–(C11) need to be solved to obtain the association probabilities and therefore the cluster distribution. Either this can be done numerically all together or one can solve Eqs. (C8) and (C9) together to obtain the association probabilities $p_{+c/c+}$ as a function of ϕ_+^c, and Eqs. (C10) and (C11) to obtain association probabilities $p_{+i/i+}$ as a function of ϕ_+^i. These resulting probability equations, which are functions of ϕ_+^c and ϕ_+^i, need to be self-consistently solved to find the consistent values of the association probabilities.

Instead of solving the set of equations in its full complexity, we only study a single limiting case. We take $\Lambda_c \gg \Lambda_i$. Therefore, practically all of the chelating agents are bound to the cations. This means that $p_{c+} = 1$ and $p_{+c} = \phi_c / \phi_+ < 1$ from the conservation of associations. Therefore, $\phi_+^i = \phi_+ - \phi_c$, which is a known quantity, and

can be used in Eqs. (C10) and (C11) to obtain association probabilities $p_{+i/i+}$.

Let us again study the limit of the sticky cation approximation, given by Eqs. (A2) and (A3), but where one of the solvents is replaced by anions. Again, let us start from a HCE $(1 = \phi_+ + \phi_- + \phi_x)$ and add the chelating agent, and see how the association probabilities change between these two systems. The chelating agent reduces the overall volume fraction of all other species, but from LHCEs we know that this does not alter the association probabilities, provided $\tilde{\Lambda}$ is constant. Relative to the HCE without the chelating agent, the new volume fraction of anions is given by $\phi_-' = \phi_-(1 - \phi_c)$ and the new volume fraction of the solvent by $\phi_x' = \phi_x(1 - \phi_c)$, while the new volume fraction of cations is give by $\phi_+' = \phi_+(1 - \phi_c) - \phi_c$, assuming that all the chelating agent binds to the cation.

We find that (assuming equal volumes and numbers for everything, $\phi_+ = \phi_- = \phi_x$ and $c_+ = c_- = c_x$, $f_+ = 4$, $f_- = 3$, which is typical), for solvent-cation associations favored over the anion-cation associations, $\tilde{\Lambda} = \Lambda_- / \Lambda_x < 1$, the addition of the chelating agent causes reductions in both p_{+-} and p_{-+}, which clearly reduces $p_{+-} p_{-+}$ and the extent of large clusters. There is an increase in p_{+x} to compensate for the decreased p_{+-} (because of the sticky cation approximation), and a decrease in p_{x+} from the conservation of associations. Therefore, the chelating agent breaks up the aggregates. On the other hand, for $\tilde{\Lambda} = \Lambda_- / \Lambda_x > 1$, the addition of the chelating agents increases p_{+-} but decreases p_{-+}, and results in both p_{+x} and p_{x+} decreasing. The increase in p_{+-} is small in comparison to the decrease in p_{-+}, which means that $p_{+-} p_{-+}$ decreases and breaks up larger clusters in favor of smaller ones.

Therefore, it appears that it is always advantageous to introduce a chelating agent to break up large clusters [143, 144], and the design principle of adding these molecules is supported by our theory [145].

APPENDIX D: CONSISTENT REPORTING OF ASSOCIATIONS

Molecular dynamics simulations (classical and ab initio) are often the method of choice for understanding non-aqueous electrolytes, but the quantities that are reported from such simulations often differ, making it difficult to compare two studies. For example, sometimes the percentages of $0, 1, 2, 3, \ldots$ anions coordinated to the cation are shown, or the percentage of the free or bound solvent, pictures of percolating aggregates, or the numbers or frequency of certain coordination environments are reported. This inconsistency in reporting the associations makes it difficult to systematically compare studies, and often not enough information is provided to fully characterize the associations. Here we outline a convention for reporting associations, as the developed theory provides a framework to make reporting such results more systematic.

As is usually done in some form already, the ensemble average coordination number of species j associated with species i, $\mathcal{N}_{ij}$, should be stated (note that index i was dropped in the main text, as only the coordination shell of cations was considered). This information can be used to calculate or infer the functionality of each species f_i, as the sum of the average coordination numbers should be a maximum of f_i (within some tolerance). The $\mathcal{N}_{ij}$ can also be used to calculate the association probabilities using the f_i through $p_{ij} = \mathcal{N}_{ij}/f_i$, or from the conservation of associations and the volume fractions. While this is a natural starting point, only reporting the directly associated species does not always uniquely characterize all the clusters, and it is usually necessary to calculate further quantities.

A requirement of our theory is that only two species can have functionalities larger than 1, with all other species only being allowed functionalities of 1. This requirement is a reflection of the fact that if there are three species with functionalities larger than 1, the Cayley tree clusters are no longer uniquely defined by their rank. So far, we have only worked with electrolytes within this requirement, but it is clear that the promising properties of high entropy electrolytes will mean studying compositions outside of this requirement.

For the case of a maximum of two species with a functionality larger than 1, if the electrolyte (almost) exclusively forms Cayley tree clusters, the clusters are uniquely defined by their rank and the cluster distribution $c_{lmsq\cdots}$ can be reported. To display the cluster distribution of this case, two-dimensional (2D) maps of the $c_{lm} = \sum_{sq\cdots} c_{lmsq\cdots}$ should be displayed, where l and m are the species that can percolate ($f_i > 1$), and $sq\cdots$ have $f_i = 1$. In addition, as single cation species are presumably of most interest (as aggregates with more than one cation are typically large and immobile), 2D concentration plots over different combinations of anion-solvents or solvent-solvent would clearly show these clusters of most interest. If the inequality $p_{ij}p_{ji} < (f_j - 1)(f_i - 1)$ holds, the system is in the pregel regime. If $p_{ij}p_{ji} \geqslant (f_j - 1)(f_i - 1)$, the system is in the postgel regime, and in addition to the cluster distribution being specified, the fraction of each species in the gel must also be stated.

Crucially, to test if Cayley tree clusters are formed, the cluster bond density can be calculated through the number of associations in a cluster divided by the number of species in that cluster. For Cayley trees, the cluster bond density is $1 - 1/N$, where N is the number of species in the cluster. For very large clusters, the cluster bond density of Cayley trees saturates at 1. If the cluster bond density (substantially) exceeds $1 - 1/N$ then there are (significant) intracluster loops, indicating that more ordered aggregates than Cayley trees are formed. If this is the case, the cluster distribution $c_{lmsq\cdots}$ no longer uniquely defines the system, and for each cluster of rank $lmsq\cdots$, there exists another distribution on how this cluster is connected (with different numbers of associations to different species), which must be specified to uniquely define the system. While it is unclear exactly how these results should be reported from our theory (and we hope that future work will make this more clear), we believe that reporting results just based on the rank of the cluster still provides valuable information, following the previously suggested plots, and would be a good starting point to quantifying the clusters.

If there are more than two species with functionalities larger than 2, even if Cayley tree clusters are formed, the rank of the cluster does not uniquely define the cluster. Therefore, how the clusters are connected must always be reported for this case. It is still important to calculate the cluster bond density, as this information provides insight into how ordered clusters are. Again, as it is unclear from the theory exactly how to present the results of these clusters, we suggest that the convention of two species with $f_i > 1$ is followed, but where all of the relevant two-species combinations is displayed on a 2D plot. Similarly, the volume fraction of each species in the gel should be reported, if present.

---

[1] K. Xu, Nonaqueous liquid electrolytes for lithium-based rechargeable batteries, Chem. Rev. **104**, 4303 (2004).

[2] K. Xu, Electrolytes and interphases in Li-ion batteries and beyond, Chem. Rev. **114**, 11503 (2014).

[3] J. Zheng, J. A. Lochala, A. Kwok, Z. D. Deng, and J. Xiao, Research progress towards understanding the unique interfaces between concentrated electrolytes and electrodes for energy storage applications, Adv. Sci. **4**, 1700032 (2017).

[4] M. Li, C. Wang, Z. Chen, K. Xu, and J. Lu, New concepts in electrolytes, Chem. Rev. **120**, 6783 (2020).

[5] Y. Tian, G. Zeng, A. Rutt, T. Shi, H. Kim, J. Wang, J. Koettgen, Y. Sun, B. Ouyang, T. Chen, Z. Lun, Z. Rong, K. Persson, and G. Ceder, Promises and challenges of next-generation "beyond Li-ion" batteries for electric vehicles and grid decarbonization, Chem. Rev. **121**, 1623 (2021).

[6] K. Xu, Navigating the minefield of battery literature, Commun. Mater. **3**, 31 (2022).

[7] Z. Piao, R. Gao, Y. Liu, G. Zhou, and H.-M. Cheng, A review on regulating Li$^+$ solvation structures in carbonate electrolytes for lithium metal batteries, Adv. Mater., 2206009 (2023).

[8] H. Cheng, Q. Sun, L. Li, Y. Zou, Y. Wang, T. Cai, F. Zhao, G. Liu, Z. Ma, W. Wahyudi, Q. Li, and J. Ming, Emerging era of electrolyte solvation structure and interfacial model in batteries, ACS Energy Lett. **7**, 490 (2022).

[9] W. Li, E. M. Erickson, and A. Manthiram, High-nickel layered oxide cathodes for lithium-based automotive batteries, Nat. Energy **5**, 26 (2020).

[10] J. Chen, X. Fan, Q. Li, H. Yang, M. R. Khoshi, Y. Xu, S. Hwang, L. Chen, X. Ji, and C. Yang, *et al.*, Electrolyte design for LiF-rich solid–electrolyte interfaces to enable

high-performance microsized alloy anodes for batteries, Nat. Energy **5**, 386 (2020).

[11] H. Wang, Z. Yu, X. Kong, S. C. Kim, D. T. Boyle, J. Qin, Z. Bao, and Y. Cui, Liquid electrolyte: The nexus of practical lithium metal batteries, Joule **6**, 588 (2022).

[12] Z. Yu, H. Wang, X. Kong, W. Huang, Y. Tsao, D. G. Mackanic, K. Wang, X. Wang, W. Huang, and S. Choudhury, *et al.*, Molecular design for electrolyte solvents enabling energy-dense and long-cycling lithium metal batteries, Nat. Energy **5**, 526 (2020).

[13] Z. Yu, P. E. Rudnicki, Z. Zhang, Z. Huang, H. Celik, S. T. Oyakhire, Y. Chen, X. Kong, S. C. Kim, and X. Xiao, *et al.*, Rational solvent molecule tuning for high-performance lithium metal battery electrolytes, Nat. Energy **7**, 94 (2022).

[14] L. Qin, N. Xiao, J. Zheng, Y. Lei, D. Zhai, and Y. Wu, Localized high-concentration electrolytes boost potassium storage in high-loading graphite, Adv. Energy Mater. **9**, 1902618 (2019).

[15] J. Zheng, S. Chen, W. Zhao, J. Song, M. H. Engelhard, and J.-G. Zhang, Extremely stable sodium metal batteries enabled by localized high-concentration electrolytes, ACS Energy Lett. **3**, 315 (2018).

[16] S. Chen, Q. Nian, L. Zheng, B.-Q. Xiong, Z. Wang, Y. Shen, and X. Ren, Highly reversible aqueous zinc metal batteries enabled by fluorinated interphases in localized high concentration electrolytes, J. Mater. Chem. A **9**, 22347 (2021).

[17] Y. Xie, J. Wang, B. H. Savitzky, Z. Chen, Y. Wang, S. Betzler, K. Bustillo, K. Persson, Y. Cui, L.-W. Wang, C. Ophus, P. Ercius, and H. Zheng, Spatially resolved structural order in low-temperature liquid electrolyte, Sci. Adv. **9**, eadc9721 (2023).

[18] K. Xu, Y. Lam, S. S. Zhang, T. R. Jow, and T. B. Curtis, Solvation sheath of Li$^+$ in nonaqueous electrolytes and its implication of graphite/electrolyte interface chemistry, J. Phys. Chem. C **111**, 7411 (2007).

[19] A. von Wald Cresce, O. Borodin, and K. Xu, Correlating Li$^+$ solvation sheath structure with interphasial chemistry on graphite, J. Phys. Chem. C **116**, 26111 (2012).

[20] O. Borodin, J. Self, K. A. Persson, C. Wang, and K. Xu, Uncharted waters: Super-concentrated electrolytes, Joule **4**, 69 (2020).

[21] R. Andersson, F. Årén, A. A. Franco, and P. Johansson, Ion transport mechanisms via time-dependent local structure and dynamics in highly concentrated electrolytes, J. Electrochem. Soc. **167**, 140537 (2020).

[22] H. Wang, S. C. Kim, T. Rojas, Y. Zhu, Y. Li, L. Ma, K. Xu, A. T. Ngo, and Y. Cui, Correlating Li-ion solvation structures and electrode potential temperature coefficients, J. Am. Chem. Soc. **143**, 2264 (2021).

[23] S. C. Kim, X. Kong, R. A. Vilá, W. Huang, Y. Chen, D. T. Boyle, Z. Yu, H. Wang, Z. Bao, J. Qin, and Y. Cui, Potentiometric measurement to probe solvation energy and its correlation to lithium battery cyclability, J. Am. Chem. Soc. **143**, 10301 (2021).

[24] L. Suo, Y.-S. Hu, H. Li, M. Armand, and L. Chen, A new class of solvent-in-salt electrolyte for high-energy rechargeable metallic lithium batteries, Nat. Commun. **4**, 1481 (2013).

[25] Y. Chen, Z. Yu, P. Rudnicki, H. Gong, Z. Huang, S. C. Kim, J.-C. Lai, X. Kong, J. Qin, Y. Cui, and Z. Bao, Steric effect tuned ion solvation enabling stable cycling of high-voltage lithium metal battery, J. Am. Chem. Soc. **143**, 18703 (2021).

[26] S. Chen, J. Zheng, D. Mei, K. S. Han, M. H. Engelhard, W. Zhao, W. Xu, J. Liu, and J.-G. Zhang, High-voltage lithium-metal batteries enabled by localized high-concentration electrolytes, Adv. Mater. **30**, 1706102 (2018).

[27] X. Ren, S. Chen, H. Lee, D. Mei, M. H. Engelhard, S. D. Burton, W. Zhao, J. Zheng, Q. Li, M. S. Ding, M. Schroeder, J. Alvarado, K. Xu, Y. S. Meng, J. Liu, J.-G. Zhang, and W. Xu, Localized high-concentration sulfone electrolytes for high-efficiency lithium-metal batteries, Chem **4**, 1877 (2018).

[28] X. Cao, H. Jia, W. Xu, and J.-G. Zhang, localized high-concentration electrolytes for lithium batteries, J. Electrochem. Soc. **168**, 010522 (2021).

[29] J. Liu, B. Yuan, L. Dong, S. Zhong, Y. Ji, Y. Liu, J. Han, C. Yang, and W. He, Constructing low-solvation electrolytes for next- generation lithium-ion batteries, Batteries Supercaps **5**, e202200256 (2022).

[30] V. Koch and J. Young, The stability of the secondary lithium electrode in tetrahydrofuran-based electrolytes, J. Electrochem. Soc. **125**, 1371 (1978).

[31] V. R. Koch, J. L. Goldman, C. J. Mattos, and M. Mulvaney, Specular lithium deposits from lithium hexafluoroarsenate/diethyl ether electrolytes, J. Electrochem. Soc. **129**, 1 (1982).

[32] J. Foos and T. Stolki, A new ether solvent for lithium cells, J. Electrochem. Soc. **135**, 2769 (1988).

[33] J. Qian, W. A. Henderson, W. Xu, P. Bhattacharya, M. Engelhard, O. Borodin, and J.-G. Zhang, High rate and stable cycling of lithium metal anode, Nat. Commun. **6**, 1 (2015).

[34] J. Barthel, R. Buchner, and E. Wismeth, FTIR spectroscopy of ion solvation of LiClO$_4$ and LiSCN in acetonitrile, benzonitrile, and propylene carbonate, J. Solut. Chem. **29**, 937 (2000).

[35] A. V. Cresce, S. M. Russell, O. Borodin, J. A. Allen, M. A. Schroeder, M. Dai, J. Peng, M. P. Gobet, S. G. Greenbaum, R. E. Rogers, and K. Xu, Solvation behavior of carbonate-based electrolytes in sodium ion batteries, Phys. Chem. Chem. Phys. **19**, 574 (2017).

[36] D. M. Seo, O. Borodin, S.-D. Han, Q. Ly, P. D. Boyle, and W. A. Henderson, Electrolyte solvation and ionic association, J. Electrochem. Soc. **159**, A553 (2012).

[37] D. M. Seo, O. Borodin, S.-D. Han, P. D. Boyle, and W. A. Henderson, Electrolyte solvation and ionic association II. Acetonitrile-lithium salt mixtures: Highly dissociated salts, J. Electrochem. Soc. **159**, A1489 (2012).

[38] L. Yang, A. Xiao, and B. L. Lucht, Investigation of solvation in lithium ion battery electrolytes by NMR spectroscopy, J. Mol. Liq. **154**, 131 (2010).

[39] Y. Zhang, M. Su, X. Yu, Y. Zhou, J. Wang, R. Cao, W. Xu, C. Wang, D. R. Baer, O. Borodin, K. Xu, Y. Wang, X.-L. Wang, Z. Xu, F. Wang, and Z. Zhu, Investigation of ion-solvent interactions in nonaqueous electrolytes using in situ liquid sims, Anal. Chem. **90**, 3341 (2018).

[40] O. O. Postupna, Y. V. Kolesnik, O. N. Kalugin, and O. V. Prezhdo, Microscopic structure and dynamics of LiBF$_4$ solutions in cyclic and linear carbonates, J. Phys. Chem. B **115**, 14563 (2011).

[41] O. Borodin and D. Bedrov, Interfacial structure and dynamics of the lithium alkyl dicarbonate SEI components in contact with the lithium battery electrolyte, J. Phys. Chem. C **118**, 18362 (2014).

[42] Z. Li, O. Borodin, G. D. Smith, and D. Bedrov, Effect of organic solvents on Li$^+$ ion solvation and transport in ionic liquid electrolytes: A molecular dynamics simulation study, J. Phys. Chem. B **119**, 3085 (2015).

[43] I. Skarmoutsos, V. Ponnuchamy, V. Vetere, and S. Mossa, Li$^+$ solvation in pure, binary, and ternary mixtures of organic carbonate electrolytes, J. Phys. Chem. C **119**, 4502 (2015).

[44] O. Borodin, X. Ren, J. Vatamanu, A. von Wald Cresce, J. Knap, and K. Xu, Modeling insight into battery electrolyte electrochemical stability and interfacial structure, Acc. Chem. Res. **50**, 2886 (2017).

[45] S. Han, A salient effect of density on the dynamics of nonaqueous electrolytes, Sci. Rep. **7**, 46718 (2017).

[46] B. Ravikumar, M. Mynam, and B. Rai, Effect of salt concentration on properties of lithium ion battery electrolytes: A molecular dynamics study, J. Phys. Chem. C **122**, 8173 (2018).

[47] Y. Shim, Computer simulation study of the solvation of lithium ions in ternary mixed carbonate electrolytes: Free energetics, dynamics, and ion transport, Phys. Chem. Chem. Phys. **20**, 28649 (2018).

[48] S. Han, Structure and dynamics in the lithium solvation shell of nonaqueous electrolytes, Sci. Rep. **9**, 5555 (2019).

[49] N. Piao, X. Ji, H. Xu, X. Fan, L. Chen, S. Liu, M. N. Garaga, S. G. Greenbaum, L. Wang, C. Wang, and X. He, Countersolvent electrolytes for lithium-metal batteries, Adv. Energy Mater. **10**, 1903568 (2020).

[50] T. Hou, K. D. Fong, J. Wang, and K. A. Persson, The solvation structure, transport properties and reduction behavior of carbonate-based electrolytes of lithium-ion batteries, Chem. Sci. **12**, 14740 (2021).

[51] Y. Wu, A. Wang, Q. Hu, H. Liang, H. Xu, L. Wang, and X. He, Significance of antisolvents on solvation structures enhancing interfacial chemistry in localized high-concentration electrolytes, ACS Cent. Sci. **8**, 1290 (2022).

[52] S. P. Beltran, X. Cao, J.-G. Zhang, and P. B. Balbuena, Localized high concentration electrolytes for high voltage lithium-metal batteries: Correlation between the electrolyte composition and its reductive/oxidative stability, Chem. Mater. **32**, 5973 (2020).

[53] I.-B. Magdău, D. J. Arismendi-Arrieta, H. E. Smith, C. P. Grey, K. Hermansson, and G. Csányi, Machine learning force field for molecular liquids: EC/EMC binary solvent, (2022), https://doi.org/10.26434/chemrxiv-2022-l4tb9.

[54] N. Yao, X. Chen, Z.-H. Fu, and Q. Zhang, Applying classical, ab initio, and machine-learning molecular dynamics simulations to the liquid electrolyte for rechargeable batteries, Chem. Rev. **122**, 10970 (2022).

[55] M. McEldrew, Z. A. H. Goodwin, S. Bi, M. Z. Bazant, and A. A. Kornyshev, Theory of ion aggregation and gelation in super-concentrated electrolytes, J. Chem. Phys. **152**, 234506 (2020).

[56] M. McEldrew, Z. A. H. Goodwin, H. Zhao, M. Z. Bazant, and A. A. Kornyshev, Correlated ion transport and the gel phase in room temperature ionic liquids, J. Phys. Chem. B **125**, 2677 (2021).

[57] M. McEldrew, Z. A. H. Goodwin, S. Bi, A. A. Kornyshev, and M. Z. Bazant, Ion clusters and networks in water-in-salt electrolytes, J. Electrochem. Soc. **168**, 050514 (2021).

[58] M. McEldrew, Z. A. H. Goodwin, N. Molinari, B. Kozinsky, A. A. Kornyshev, and M. Z. Bazant, Salt-in-ionic-liquid electrolytes: Ion network formation and negative effective charges of alkali metal cations, J. Phys. Chem. B **125**, 13752 (2021).

[59] P. J. Flory, Molecular size distribution in three dimensional polymers. I. Gelation, J. Am. Chem. Soc. **63**, 3083 (1941).

[60] P. J. Flory, Molecular size distribution in three dimensional polymers. II. Trifunctional branching units, J. Am. Chem. Soc. **63**, 3091 (1941).

[61] P. J. Flory, Constitution of three-dimensional polymers and the theory of gelation, J. Phys. Chem. **46**, 132 (1942).

[62] P. J. Flory, Thermodynamics of high polymer solutions, J. Chem. Phys. **10**, 51 (1942).

[63] P. J. Flory, *Principles of Polymer Chemistry* (Cornell University Press, Ithaca, New York, 1953).

[64] P.-J. Flory, Statistical thermodynamics of semi-flexible chain molecules, Proc. Math. Phys. Eng. **234**, 60 (1956).

[65] W. H. Stockmayer, Theory of molecular size distribution and gel formation in branched-chain polymers, J. Chem. Phys. **11**, 45 (1943).

[66] W. H. Stockmayer, Theory of molecular size distribution and gel formation in branched polymers II. General cross linking, J. Chem. Phys. **12**, 125 (1944).

[67] W. H. Stockmayer, Molecular distribution in condensation polymers, J. Polym. Sci. **9**, 69 (1952).

[68] F. Tanaka, Theory of thermoreversible gelation, Macromolecules **22**, 1988 (1989).

[69] F. Tanaka, Thermodynamic theory of network-forming polymer solutions. 1, Macromolecules **23**, 3784 (1990).

[70] F. Tanaka and W. H. Stockmayer, Thermoreversible gelation with junctions of variable multiplicity, Macromolecules **27**, 3943 (1994).

[71] M. Ishida and F. Tanaka, Theoretical study of the postgel regime in thermoreversible gelation, Macromolecules **30**, 3900 (1997).

[72] F. Tanaka and M. Ishida, Thermoreversible gelation of hydrated polymers, J. Chem. Soc. Faraday Trans. **91**, 2663 (1995).

[73] F. Tanaka, Thermoreversible gelation of associating polymers, Phys. A: Stat. Mech. Appl. **257**, 245 (1998).

[74] F. Tanaka, Theoretical study of molecular association and thermoreversible gelation in polymers, Polym. J. **34**, 479 (2002).

[75] F. Tanaka and M. Ishida, Thermoreversible gelation with two-component networks, Macromolecules **32**, 1271 (1999).

[76] F. Tanaka, *Polymer Physics: Applications to Molecular Association and Thermoreversible Gelation* (Cambridge University Press, New York, 2011).

[77] J. G. Kirkwood, Statistical mechanics of liquid solutions, Chem. Rev. **19**, 275 (1936).

[78] A. Levy, M. McEldrew, and M. Z. Bazant, Spin-glass charge ordering in ionic liquids, Phys. Rev. Mater. **3**, 055606 (2019).

[79] K. S. Pitzer, Critical phenomena in ionic fluids, Acc. Chem. Res. **23**, 333 (1990).

[80] K. S. Pitzer, *Activity Coefficients in Electrolyte Solutions* (CRC Press, Boca Raton, 1991), 2nd ed.

[81] M. E. Fisher, The story of coulombic criticality, J. Stat. Phys. **75**, 1 (1994).

[82] A. Z. Panagiotopoulos and M. E. Fisher, Phase Transitions in 2:1 and 3:1 Hard-Core Model Electrolytes, Phys. Rev. Lett. **88**, 045701 (2002).

[83] Q. Yan and J. J. de Pablo, Phase Equilibria of Charge-, Size-, and Shape-Asymmetric Model Electrolytes, Phys. Rev. Lett. **88**, 095504 (2002).

[84] K. V. Workum and J. F. Douglas, Symmetry, equivalence, and molecular self-assembly, Phys. Rev. E **73**, 031502 (2006).

[85] J. Dudowicz, K. F. Freed, and J. F. Douglas, Flory-Huggins Model of Equilibrium Polymerization and Phase Separation in the Stockmayer Fluid, Phys. Rev. Lett. **92**, 045502 (2004).

[86] J. C. Shelley and G. N. Patey, A comparison of liquid–vapor coexistence in charged hard sphere and charged hard dumbbell fluids, J. Chem. Phys. **103**, 8299 (1995).

[87] S. Bastea, Living polymers in a size-asymmetric electrolyte, Phys. Rev. E **66**, 020801(R) (2002).

[88] J. P. K. Doye and D. J. Wales, Structural transitions and global minima of sodium chloride clusters, Phys. Rev. B **59**, 2292 (1999).

[89] Z. Yu, N. P. Balsara, O. Borodin, A. A. Gewirth, N. T. Hahn, E. J. Maginn, K. A. Persson, V. Srinivasan, M. F. Toney, K. Xu, K. R. Zavadil, L. A. Curtiss, and L. Cheng, Beyond local solvation structure: Nanometric aggregates in battery electrolytes and their effect on electrolyte properties, ACS Energy Lett. **7**, 461 (2022).

[90] J.-H. Choi and M. Cho, Ion aggregation in high salt solutions. II. Spectral graph analysis of water hydrogen-bonding network and ion aggregate structures, J. Chem. Phys. **141**, 154502 (2014).

[91] J.-H. Choi and M. Cho, Ion aggregation in high salt solutions. IV. Graph-theoretical analyses of ion aggregate structure and water hydrogen bonding network, J. Chem. Phys. **143**, 104110 (2015).

[92] J.-H. Choi, H. Kim, S. Kim, S. Lim, B. Chon, and M. Cho, Ion aggregation in high salt solutions. III. Computational vibrational spectroscopy of hdo in aqueous salt solutions, J. Chem. Phys. **142**, 204102 (2015).

[93] J.-H. Choi, H. R. Choi, J. Jeon, and M. Cho, Ion aggregation in high salt solutions. VII. The effect of cations on the structures of ion aggregates and water hydrogen-bonding network, J. Chem. Phys. **147**, 154107 (2017).

[94] R. Demichelis, P. Raiteri, J. D. Gale, D. Quigley, and D. Gebauer, Stable prenucleation mineral clusters are liquid-like ionic polymers, Nat. Commun. **2**, 590 (2011).

[95] M. E. Cates and S. J. Candau, Statics and dynamics of worm-like surfactant micelles, J. Phys.: Condens. Matter **2**, 6869 (1990).

[96] S. K. Kumar and J. F. Douglas, Gelation in Physically Associating Polymer Solutions, Phys. Rev. Lett. **87**, 188301 (2001).

[97] I. Saika-Voivod, E. Zaccarelli, F. Sciortino, S. V. Buldyrev, and P. Tartaglia, Effect of bond lifetime on the dynamics of a short-range attractive colloidal system, Phys. Rev. E **70**, 041401 (2004).

[98] E. Zaccarelli, S. Buldyrev, E. La Nave, A. Moreno, I. Saika-Voivod, F. Sciortino, and P. Tartaglia, Model for Reversible Colloidal Gelation, Phys. Rev. Lett. **94**, 218301 (2005).

[99] E. Zaccarelli, Colloidal gels: Equilibrium and non-equilibrium routes, J. Phys. Condens. Matter **19**, 323101 (2007).

[100] J. Russo, P. Tartaglia, and F. Sciortino, Reversible gels of patchy particles: Role of the valence, J. Chem. Phys. **131**, 014504 (2009).

[101] S. Corezzi, C. De Michele, E. Zaccarelli, P. Tartaglia, and F. Sciortino, Connecting irreversible to reversible aggregation: Time and temperature, J. Phys. Chem. B **113**, 1233 (2009).

[102] F. Smallenburg and F. Sciortino, Liquids more stable than crystals in particles with limited valence and flexible bonds, Nat. Phys. **9**, 554 (2013).

[103] E. Bianchi, P. Tartaglia, E. Zaccarelli, and F. Sciortino, Theoretical and numerical study of the phase diagram of patchy colloids: Ordered and disordered patch arrangements, J. Chem. Phys. **128**, 144504 (2008).

[104] E. Bianchi, P. Tartaglia, E. L. Nave, and F. Sciortino, Fully solvable equilibrium self-assembly process: Fine-tuning the clusters size and the connectivity in patchy particle systems, J. Phys. Chem. B **111**, 11765 (2007).

[105] F. Sciortino, E. Bianchi, J. F. Douglas, and P. Tartaglia, Self-assembly of patchy particles into polymer chains: A parameter-free comparison between Wertheim theory and Monte Carlo simulation, J. Chem. Phys. **126**, 194903 (2007).

[106] D. J. Audus, F. W. Starr, and J. F. Douglas, Coupling of isotropic and directional interactions and its effect on phase separation and self-assembly, J. Chem. Phys. **144**, 074901 (2016).

[107] D. J. Audus, F. W. Starr, and J. F. Douglas, Valence, loop formation and universality in self-assembling patchy particles, Soft Matter **14**, 1622 (2018).

[108] A. Gröschel, A. Walther, T. I. Löbling, F. H. Schacher, H. Schmalz, and A. H. E. Müller, Guided hierarchical co-assembly of soft patchy nanoparticles, Nature **503**, 247 (2013).

[109] A. M. Kalsin, B. Kowalczyk, S. K. Smoukov, R. Klajn, and B. A. Grzybowski, Ionic-like behavior of oppositely charged nanoparticles, J. Am. Chem. Soc. **128**, 15046 (2006).

[110] A. M. Kalsin and B. A. Grzybowski, Controlling the growth of "ionic" nanoparticle supracrystals, Nano Lett. **7**, 1018 (2007).

[111] A. Umar and S.-M. Choi, Aggregation behavior of oppositely charged gold nanorods in aqueous solution, J. Phys. Chem. C **117**, 11738 (2013).

[112] J.-H. Choi, H. Lee, H. R. Choi, and M. Cho, Graph theory and ion and molecular aggregation in aqueous solutions, Annu. Rev. Phys. Chem. **69**, 125 (2018).

[113] Z. A. H. Goodwin, M. McEldrew, J. de Souza, M. Z. Bazant, and A. A. Kornyshev, Gelation, clustering and crowding in the electrical double layer of ionic liquids, J. Chem. Phys. **157**, 094106 (2022).

[114] T. R. Kartha and B. S. Mallik, Molecular dynamics and emerging network graphs of interactions in dinitrile-based Li-ion battery electrolytes, J. Phys. Chem. B **125**, 7231 (2021).

[115] Z. A. H. Goodwin and A. A. Kornyshev, Cracking ion pairs in the electrical double layer of ionic liquids, Electrochim. Acta **434**, 141163 (2022).

[116] Z. A. H. Goodwin and A. A. Kornyshev, Underscreening, overscreening and double-layer capacitance, Electrochem. Commun. **82**, 129 (2017).

[117] M. Chen, Z. A. H. Goodwin, G. Feng, and A. A. Kornyshev, On the temperature dependence of the double layer capacitance of ionic liquids, J. Electroanal. Chem. **819**, 347 (2018).

[118] G. Feng, M. Chen, S. Bi, Z. A. H. Goodwin, E. B. Postnikov, N. Brilliantov, M. Urbakh, and A. A. Kornyshev, Free and Bound States of Ions in Ionic Liquids, Conductivity, and Underscreening Paradox, Phys. Rev. X **9**, 021024 (2019).

[119] M. S. Wertheim, Fluids with highly directional attractive forces. I. Statistical thermodynamics, J. Sat. Phys. **35**, 19 (1984).

[120] M. S. Wertheim, Fluids with highly directional attractive forces. II. Thermodynamic perturbation theory and integral equations, J. Sat. Phys. **35**, 35 (1984).

[121] M. S. Wertheim, Fluids with highly directional attractive forces. III. Multiple attraction sites, J. Sat. Phys. **42**, 459 (1986).

[122] M. S. Wertheim, Fluids with highly directional attractive forces. IV. Equilibrium polymerization, J. Sat. Phys. **42**, 477 (1986).

[123] P. I. C. Teixeira and F. Sciortino, Patchy particles at a hard wall: Orientation dependent bonding, J. Chem. Phys. **151**, 174903 (2019).

[124] H. Liu, S. K. K. F. Sciortino, and G. T. Evans, Vapor-liquid coexistence of fluids with attractive patches: An application of Wertheim's theory of association, J. Chem. Phys. **130**, 044902 (2009).

[125] Y. Marcus and G. Hefter, Ion pairing, Chem. Rev. **106**, 4585 (2006).

[126] S. Plimpton, Fast parallel algorithms for short-range molecular dynamics, J. Comput. Phys. **117**, 1 (1995).

[127] A. P. Thompson, H. M. Aktulga, R. Berger, D. S. Bolintineanu, W. M. Brown, P. S. Crozier, P. J. in 't Veld, A. Kohlmeyer, S. G. Moore, T. D. Nguyen, M. J. S. R. Shan, J. Tranchida, C. Trott, and S. J. Plimpton, LAMMPS - a flexible simulation tool for particle-based materials modeling at the atomic, meso, and continuum scales, Comp. Phys. Commun. **271**, 10817 (2022).

[128] L. Martínez, R. Andrade, E. G. Birgin, and J. M. Martínez, Packmol: A package for building initial configurations for

[129] J. N. C. Lopes and A. A. Pádua, CL&P: A generic and systematic force field for ionic liquids modeling, Theor. Chem. Acc. **131**, 1129 (2012).

[130] W. L. Jorgensen, D. S. Maxwell, and J. Tirado-Rives, Development and testing of the OPLS all-atom force field on conformational energetics and properties of organic liquids, J. Am. Chem. Soc. **118**, 11225 (1996).

[131] W. L. Jorgensen and J. Tirado-Rives, Potential energy functions for atomic-level simulations of water and organic and biomolecular systems, PNAS **102**, 6665 (2005).

[132] L. S. Dodda, J. Z. Vilseck, J. Tirado-Rives, and W. L. Jorgensen, 1.14*CM1A-LBCC: Localized bond-charge corrected cm1a charges for condensed-phase simulations, J. Phys. Chem. B **121**, 3864 (2017).

[133] L. S. Dodda, I. C. de Vaca, J. Tirado-Rives, and W. L. Jorgensen, LigParGen web server: An automatic OPLS-AA parameter generator for organic ligands, Nucleic Acids Res. Spec. Publ. **45**, W331 (2017).

[134] J. Xu, J. Zhang, T. P. Pollard, Q. Li, S. Tan, S. Hou, H. Wan, F. Chen, H. He, E. Hu, K. Xu, X.-Q. Yang, and O. B. C. Wang, Electrolyte design for Li-ion batteries under extreme operating conditions, Nature **614**, 694 (2023).

[135] S. C. Kim, J. Wang, R. Xu, P. Zhang, Y. Chen, Z. Huang, Y. Yang, Z. Yu, S. T. Oyakhire, W. Zhang, M. S. Kim, D. T. Boyle, P. Sayavong, J. Qin, Z. Bao, and Y. Cui, High entropy electrolytes for practical lithium metal batteries, (2022), https://doi.org/10.26434/chemrxiv-2022-j40p4.

[136] Q. Wang, C. Zhao, Z. Yao, J. Wang, F. Wu, S. G. H. Kumar, S. Ganapathy, S. Eustace, X. Bai, B. Li, J. Lu, and M. Wagemaker, Entropy-driven liquid electrolytes for lithium batteries, Adv. Mater. (2023),

[137] Q. Wang, C. Zhao, J. Wang, Z. Yao, S. Wang, S. G. H. Kumar, S. Ganapathy, S. Eustace, X. Bai, B. Li, and M. Wagemaker, High entropy liquid electrolytes for lithium batteries, Nat. Commun. **14**, 440 (2023).

[138] C. Yang, *et al.*, All-temperature zinc batteries with high-entropy aqueous electrolyte, Nat. Sustain. (2023).

[139] E. P. George, D. Raabe, and R. O. Ritchie, High-entropy alloys, Nat. Rev. Mater. **4**, 515 (2019).

[140] F. Sciortino, Entropy in self-assembly, La Rivista del Nuovo Cimento **42**, 511 (2019).

[141] B. C. Rocha, S. Paul, and H. Vashisth, Role of entropy in colloidal self-assembly, Entropy **22**, 877 (2020).

[142] D. Frenkel, Order through entropy, Nat. Mater. **14**, 9 (2015).

[143] N. Molinari, J. P. Mailoa, N. Craig, J. Christensen, and B. Kozinsky, Transport anomalies emerging from strong correlation in ionic liquid electrolytes, J. Power Sources **428**, 27 (2019).

[144] N. Molinari, J. P. Mailoa, and B. Kozinsky, General trend of a negative Li$^+$ effective charge in ionic liquid electrolytes, J Phys. Chem. Lett. **10**, 2313 (2019).

[145] N. Molinari and B. Kozinsky, Chelation-induced reversal of negative cation transference number in ionic liquid electrolytes, J. Phys. Chem. B **124**, 2676 (2020).

[146] F. Sciortino, C. D. Michele, and J. F. Douglas, Growth of equilibrium polymers under non-equilibrium conditions, J. Phys.: Condens. Matter **20**, 155101 (2008).

[147] P. Tartaglia, Gel formation through reversible and irreversible aggregation, J. Phys.: Condens. Matter **21**, 504109 (2009).

[148] R. S. Hoy and G. H. Fredrickson, Thermoreversible associating polymer networks. I. Interplay of thermodynamics, chemical kinetics, and polymer physics, J. Chem. Phys. **131**, 224902 (2009).

[149] S. Corezzi, D. Fioretto, and F. Sciortino, Chemical and physical aggregation of small functionality particles, Soft Mater. **8**, 11207 (2012).

[150] W. Huang, P. M. Attia, H. Wang, S. E. Renfrew, N. Jin, S. Das, Z. Zhang, D. T. Boyle, Y. Li, M. Z. Bazant, B. D. McCloskey, W. C. Chueh, and Y. Cui, Evolution of the solid-electrolyte interphase on carbonaceous anodes visualized by atomic-resolution cryogenic electron microscopy, Nano Lett. **19**, 5140 (2019).

[151] M. B. Pinson and M. Z. Bazant, Theory of SEI formation in rechargeable batteries: Capacity fade, accelerated aging and lifetime prediction, J. Electrochim. Soc. **160**, A243 (2013).

[152] S. Das, P. M. Attia, W. C. Chueh, and M. Z. Bazant, Electrochemical kinetics of SEI growth on carbon black: Part II. Modeling, J. Electrochim. Soc. **166**, E107 (2019).

[153] B. Huang, K. H. Myint, Y. Wang, Y. Zhang, R. R. Rao, J. Sun, S. Muy, Y. Katayama, J. C. Garcia, D. Fraggedakis, J. C. Grossman, M. Z. Bazant, K. Xu, A. P. Willard, and Y. Shao-Horn, Cation-dependent interfacial structures and kinetics for outer-sphere electron-transfer reactions, J. Phys. Chem. C **125**, 4397 (2021).

[154] D. Fraggedakis, M. McEldrew, R. B. Smith, Y. Krishnan, Y. Zhang, P. Bai, W. C. Chueh, Yang Shao-Horn, and M. Z. Bazant, Theory of coupled ion-electron transfer kinetics, Electrochim. Acta **367**, 137432 (2021).

[155] F. H. Stillinger, Rigorous basis of the Frenkel-band theory of association equilibrium, J. Chem. Phys. **38**, 1486 (1963).

[156] H. C. Andersen, Cluster expansions for hydrogen bonded fluids. II. Dense liquids, J. Chem. Phys. **61**, 4985 (1974).

[157] L. Suo, O. Borodin, T. Gao, M. Olguin, J. Ho, X. Fan, C. Luo, C. Wang, and K. Xu, "Water-in-salt" electrolyte enables high-voltage aqueous lithium-ion chemistries, Science **350**, 938 (2015).

[158] D. Reber, R. Grissa, M. Becker, R.-S. Kühnel, and C. Battaglia, Anion selection criteria for water-in-salt electrolytes, Adv. Energy Mater. **11**, 2002913 (2021).

[159] Y. Yamada, K. Usui, K. Sodeyama, S. Ko, Y. Tateyama, and A. Yamada, Hydrate-melt electrolytes for high-energy-density aqueous batteries, Nat. Energy **1**, 16129 (2016).